

AD-A053 447

AIR FORCE INST OF TECH WRIGHT-PATTERSON AFB OHIO SCH--ETC F/G 1/4  
THE DESIGN OF AN OPTIMUM ALPHANUMERIC SYMBOL SET FOR COCKPIT DI--ETC(U)  
DEC 77 L F BUSH

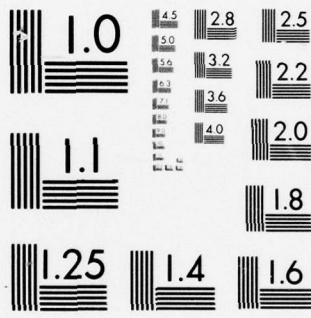
UNCLASSIFIED

AFIT/GE/EE/77-11

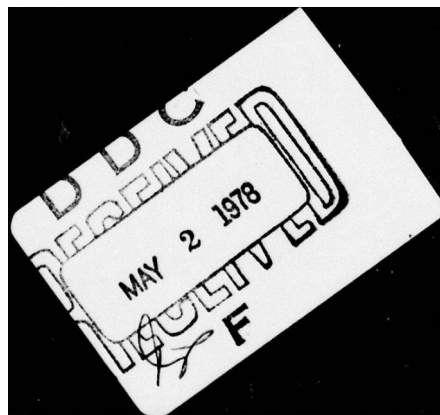
NL

1 OF 2  
AD  
A053447





MICROCOPY RESOLUTION TEST CHART  
NATIONAL BUREAU OF STANDARDS-1963-A



①

AD A 053447

DDC  
MAY 2 1978  
F

AD No. \_\_\_\_\_  
DDC FILE COPY

THE DESIGN OF AN OPTIMUM ALPHANUMERIC ✓  
SYMBOL SET FOR COCKPIT DISPLAYS

THESIS

AFIT/GE/EE/77-11 ✓

Larry F. Bush  
Capt USAF

Approved for public release; distribution unlimited.

THE DESIGN OF AN OPTIMUM ALPHANUMERIC  
SYMBOL SET FOR COCKPIT DISPLAYS

THESIS

Presented to the Faculty of the School of Engineering  
of the Air Force Institute of Technology  
Air University  
in Partial Fulfillment of the  
Requirements for the Degree of  
Master of Science

by

Larry F. Bush, B.S.

Capt USAF

Graduate Electrical Engineering

December 1977

Approved for public release; distribution unlimited.

ACCESSION for	
NTIS	WFO Section <input checked="" type="checkbox"/>
DDC	B.H. Section <input type="checkbox"/>
UNANNOUNCED	<input type="checkbox"/>
JUSTIFICATION	
BY	
DISTRIBUTION/AVAILABILITY CODES	
Dist	SP. CIAL
A	

## Preface

The research in this thesis investigates symbol shape and its association to symbol legibility. The two-dimensional Fourier transform is used to derive the feature domain and Euclidian distance is used as a basis for the symbol change procedure. The pattern recognition aspects of symbol legibility, both from an experimental and a theoretical standpoint, is crucial to the effective design of an optimum alphanumeric font.

I wish to express my gratitude to my thesis advisor, Dr. Matthew Kabrisky, Professor of Electrical Engineering, Air Force Institute of Technology, first for giving me complete autonomy during the conduct of the research, and second for his invaluable support and guidance in achieving the final product. I am also indebted to the advice and assistance I received from my sponsor, Capt. Larry G. Goble of the Air Force Flight Dynamics Laboratory (AFFDL). Special acknowledgement is given to Capt. Jim Johnson from AFFDL and to Lt. Gary Sims of the Aerospace Medical Research Laboratory for their interest and contributions to this project.

Finally, I would like to add a little more than the customary expression of appreciation to my wife Marleen for her encouragement and understanding throughout this effort.

## Contents

	<u>Page</u>
Preface .....	ii
List of Figures .....	v
List of Tables .....	vii
Abstract .....	viii
I. Introduction .....	1
II. Background .....	4
III. Methodology .....	10
Introduction .....	10
Input Symbol Representation .....	12
Fourier Analysis .....	14
Digital Computation .....	16
Spatial Filtering .....	16
Energy Normalization .....	27
Euclidian Distance .....	28
Symbol Rating .....	32
Symbol Change Procedure .....	41
Symbol Change Algorithm .....	43
Printing the Changed Symbol .....	45
IV. Testing .....	53
Subjects .....	53
Stimuli .....	53
Apparatus .....	55
Procedure .....	56
V. Results .....	58
Computer Algorithm Results .....	58
Psychophysical Testing Results .....	60
VI. Conclusions and Recommendations .....	67
Bibliography .....	71
Appendix A: Lincoln/Mitre Set .....	74
Appendix B: Final Set 11 .....	77

## Contents

	<u>Page</u>
Appendix C: ASCII, Namel, Huddleston, and IBM Sets	80
Appendix D: Fourier Transform in Fraunhofer Diffraction .....	82
Appendix E: Optimization of Legible Sets Using Distance Measure .....	88
Appendix F: Window Effect on the Distance Matrix	92
Vita .....	96

## List of Figures

<u>Figure</u>		<u>Page</u>
1	The Visual System .....	4
2	Development of Model .....	11
3	Lincoln/Mitre "A" .....	12
4	Window with Symbol Centered .....	13
5	Rearranged Fourier Real Component Array ....	17
6	1st, 2nd, 3rd, and 7th Harmonic of Window ...	18
7	9th Harmonic of Window .....	19
8	Rearranged and FOURT 3rd Harmonic Filter ...	20
9	Reproduced Symbol with 9 Repeats .....	21
10	Reproduced Symbol Using Repacked Filter ...	22
11	Repacked Filtered FOURT Array .....	23
12	Results after Filtering of L/M "P" .....	24
13	Fourier Real Array with 25 Components .....	25
14	Contrast Sensitivity for Sine-wave Grating ..	26
15	Histogram of Lincoln/Mitre Distances .....	36
16	Lincoln/Mitre Errors vs. Stimuli .....	39
17	Confusion Matrix for Lincoln/Mitre Set .....	40
18	Symbol Change Algorithm Flow Chart .....	44
19	Vector Representation of Change Equation ...	45
20	Ten Movements of Lincoln/Mitre "P" from Two Closest Neighbors .....	48
21	"P": Lincoln/Mitre and Final Set .....	47
22	Lincoln/Mitre "P" after 5 Movements with no Filter .....	49

List of Figures (Continued)

<u>Figure</u>	<u>Page</u>
23 "P" Movement from Nearest Neighbors .....	50
24 Psychophysical Testing Sequence .....	54
25 Histogram for Final Set 11 Distances .....	59
26 Cumulative Percent Correct by Trial .....	63
27 Rectangular Aperture .....	83
28 Cross Section of Fraunhofer Diffraction Pattern along X Axis .....	84
29 Fraunhofer Diffraction Setup .....	84
30 Fraunhofer Diffraction Pattern of Wire Mesh .	85
31 Restructured Wire Mesh Image .....	85
32 Horizontal Image Using Vertical Slit .....	86
33 Number "4" with Spatial Filter .....	87

## List of Tables

<u>Table</u>	<u>Page</u>
I Lincoln/Mitre Distance Matrix A-R .....	30
II Lincoln/Mitre Distance Matrix S-9 .....	31
III Lincoln/Mitre Sorted Distance Matrix A-L ..	33
IV Lincoln/Mitre Sorted Distance Matrix M-X ..	34
V Lincoln/Mitre Sorted Distance Matrix Y-9 ..	35
VI Symbol Pair Confusability Data .....	37
VII Symbol Confusability Rating .....	37
VIII Lincoln/Mitre Psychophysical Data .....	38
IX Lincoln/Mitre Ordered Mean Distance to Neighbors .....	42
X Lincoln/Mitre "P" after 10 Movements .....	51
XI Bin Number Data for Lincoln/Mitre and Final Set .....	61
XII Lincoln/Mitre and Final Set Distance to Nearest Neighbor .....	62
XIII Changed Symbols Total Errors for Both Fonts	65
XIV Symbol Algorithm .....	69
XV ASCII 10 X 14 - Ordered Distance Matrix A-L	94
XVI ASCII 30 X 42 - Ordered Distance Matrix A-L	95

Abstract

↙  
The purpose of this study was to design an alpha-numeric symbol set with improved legibility which could be implemented as a standardized set for cockpit displays. Pattern recognition theory was applied in which the two-dimensional, discrete, Fourier transform was used to obtain the feature space for each symbol. Spatial low-pass filtering techniques were employed and a decision rule was used based on the maximum nearest prototype Euclidian distance between symbols. A symbol change algorithm was developed in which symbols were moved away from their two closest neighbors in the transformed domain. Lincoln/Mitre, a highly legible font, was used as the initial prototype set. A new alphanumeric symbol set was designed with 18 changed symbols that had an overall greater distance spread between nearest neighbor symbols. The Lincoln/Mitre and a new test set were psychophysically tested with results indicating a 9.5% better performance for the changed symbols over the original Lincoln/Mitre symbols.

# THE DESIGN OF AN OPTIMUM ALPHANUMERIC SYMBOL SET FOR COCKPIT DISPLAYS

## I. Introduction

As aircraft have become more complex, there has been a concomitant increase in the number of instruments in cockpit displays. This is a consequence of the increasingly demanding performance requirements of the aircraft and the weapon systems they contain. This in turn results in a vast amount of information that must be interpreted correctly by the aircrew to insure a safe and successful mission. This is a task which is especially difficult under the high stress conditions of combat. In order to perform adequately all the requirements for a mission, the pilot and crew need flexible and dependable equipment which can display information without misinterpretation. As a result, the light-emitted diode (LED) and the cathode ray tube (CRT) are beginning to replace the mechanical gauge as a display device.

LED devices have certain favorable characteristics compared to CRT's, principally in the areas of reliability, maintainability, compactness, and logistic cost. The Air Force Flight Dynamics Laboratory (AFFDL) is presently funding research and development of green

LED matrix module display systems that may lead to revolutionary advancements in cockpit displays (Ref 19).

This thesis is concerned with the design of an optimal alphanumeric symbol set that can be implemented as a standardized set for LED displays. Current LED display units using a 10 X 14 height-to-width ratio for each symbol are being designed and tested by the AFFDL. In this study, the 10 X 14 matrix will be used as the maximum size of each symbol in the set. The matrix grid of 140 diodes (10 X 14) can contain either a charged diode which will form part of the symbol or an uncharged diode representing the background. By making slight changes in the matrix, it is possible to obtain a very large number of perfectly readable sets having differing legibility.

The objective of this thesis is to produce an alphanumeric symbol set that will achieve the most uniform distribution of errors between symbols and also decrease the overall errors in identification when compared to other fonts. A decision rule using the nearest prototype classifier based on Euclidian distance is used. A basis for this study is the discrete, two-dimensional Fourier transform that was proposed by Kabrisky as a mathematical model of the human visual information processing system (Ref 16), and used by Goble (Ref 11) to examine the distribution of errors in a letter perception test.

The Lincoln/Mitre font, one which indicated a high degree of legibility from AFFDL testing, is used as the inputted prototype set from which changes will be made to spread the distance between symbols in the set. A computer algorithm is used that centers a symbol in an array, computes Fourier coefficients, applies a low-pass filter, performs symbol change procedures, and does other related functions. Investigations are made into ways to change the dot matrix shape of the symbols that have been identified as the most confusing. Psychophysical testing procedure is described in Chapter IV with results discussed in Chapter V. A conclusion and recommendation for further study is included in Chapter VI.

## II. Background

The human eye-brain network is a pattern processing center whose vast complex functions hold many clues to the pattern recognition problem. A diagram of the visual system is shown in Figure 1 below. The primary

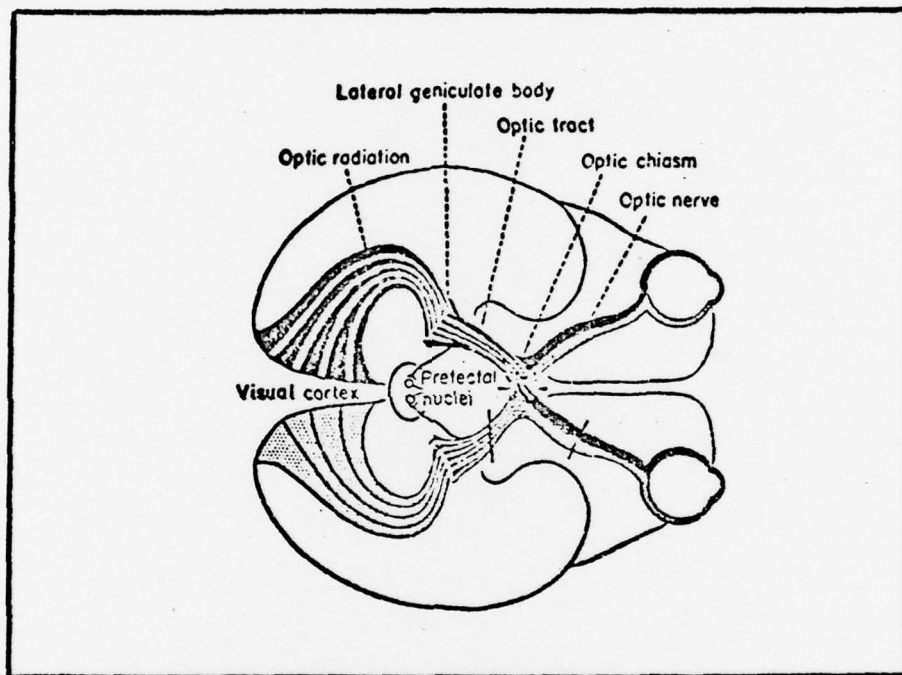


Figure 1. The Visual System. (From Ref 9:626)

parts of the human visual system consists of the retina of the eye, the optic tract, the lateral geniculate body, the cerebral cortex, and neural interconnections. The image the eye receives is focused on the back of the retina where the rods and cones act as photo sensitive receptors. The rods differ from the cones in that they

are more sensitive to light and contribute to vision at illumination levels much lower than those provided by most display panels. The cones operate at higher illumination levels, provide better contrast sensitivity and spectral resolution, and provide color vision. The response consequent to their stimulation is transferred to a matrix of retinal neurons and then to large "ganglion" cells whose output axons form the approximately one million ( $10^6$ ) channels in the optic nerve. In addition to coding the light pattern, the retina is a data reduction system for the processed image since the  $10^6$  output channels are derived from about 125 million rods and about 5.5 million cones. The two nerve tracks from each eye intersect behind the eyes, connect to the lateral geniculate bodies in the brain stem, and then go on to the cerebral cortex of the brain. The cerebral cortex is a sheet-like structure in which the flow of input-output data takes place perpendicular to the sheet. The coded visual data is mapped homomorphically onto the cortical sheet; there is a rich interconnection between neighboring areas of the cortex in which Kabrisky had theorized a two dimension Fourier transform computation could occur and characterize information transfer in the visual data processing system (Ref 16).

There has been much work done on Fourier spatial frequency analysis, as a model for the recognition of

two-dimensional images, by students at the Air Force Institute of Technology (AFIT). Radoy (Ref 20) investigated the use of Fourier transforms in which is used the low spatial frequencies of the transform to successfully classify the English alphabet. Further work by Tallman (Ref 24) verified the use of spatial low-pass filtering. Using 24 handprinted sets of the English alphabet and keeping only the first three spatial frequency harmonics, he was able to properly classify 95% of a test set which the machine had not been exposed to previously. He properly classified 99% of his training set.

Instead of a Fourier transform a two-dimensional Walsh transform was used by Carl (Ref 3) in 1969. Using Tallman's data sets, he was able to properly classify 95% of the test set within 12 training iterations. He concluded that filtering can be used to facilitate reliable machine classification.

Further work based on Kabrisky's model have been applied to a variety of pattern recognition techniques. Besides its use in the classification of handprinted alphabets (Ref 24), it has been used with Chinese characters (Ref 1), unique symbol sets (Ref 15), and in speech recognition task (Ref 6). Ginsburg (Ref 10) concluded that the model provided a means of obtaining quantitative psychological correlates of the human

visual system. Ginsburg showed that there was a relationship between human identification error and Euclidian distance when using low-pass filtered transforms of rotated letters.

The results of Goble's dissertation in 1975 supported the use of the inter-prototype Euclidian distance matrix as a model for predicting human visual perception. The distance matrix were produced from a low-pass two-dimensional discrete Fourier or Walsh transform of alphabetic characters. Small Euclidian distances represented high degree of recognition errors while the opposite was true for large Euclidian distances (Ref 11).

Legibility research has been seeking methods to determine better legible symbol sets with observer's accuracy and speed in symbol identification. There is a variety of adverse conditions under which operators read displays; such as, fatigue, stress, clutter, vibration, and symbol overprinting. The criteria that will finally rate one set better than another has to come from standardized conditions when the sets are tested using human subjects.

A contractor study was completed in 1975 for the Air Force Flight Dynamics Laboratory which investigated symbol legibility in terms of behavior data. Color, contrast, shape, percent active area, viewing angle,

symbol orientation, symbol definition, symbol subtense, vibration, translation and rotation were among the areas which influenced human perception of symbols.

The principal conclusions drawn from the study were:

1. The parameters having the major effect on display legibility are percent active area, luminance, contrast, and symbol subtense.
2. Two parameters having important interactions are symbol definition and symbol orientation.
3. For static upright symbology, there is not a performance difference for a 5 X 7 matrix or greater.
4. When a fixed matrix array is rotated, the 5 X 7 symbology was illegible, while the 8 X 11 and 10 X 21 were marginal and legible respectively (Ref 25:44,51).

Further discussion of symbolic display variables and advanced display technology can be found in Reference 21.

Over the years, several alphanumeric symbol sets have evolved that can qualify for use in electronic displays. Included among these fonts were the Lincoln/Mitre, Huddleston, Namel, ASCII, IBM 029, and Leroy. See Appendix A and C. Separate research studies conducted in comparing the legibility of different fonts

resulted in selecting the Lincoln/Mitre font as a highly legible one. Research is still lacking in developing an optimal font based on different matrix size, shape, and arrangements (Ref 25:63,65).

Recent psychophysical studies at the AFFDL have classified the Lincoln/Mitre font with the least human misidentifications. The development of the Lincoln/Mitre font began with research at Lincoln Laboratory in Lexington, Massachusetts and continues at the Mitre Corporation in Bedford, Massachusetts. It resulted from the work of several researchers over a ten year period. The Lincoln/Mitre font is well suited to use with degraded conditions and when high speed and accuracy of identification are stressed (Ref 22:42,51).

### III. Methodology

#### Introduction

The procedure in this study may be considered as a heuristic approach in which a Fourier mathematical model and spatial filtering techniques are used to find a solution to the legibility problem. Finding more legible alphanumeric symbol sets does not follow directly to the more formal pattern recognition approaches to classification, but uses pattern analysis and feature extraction to formulate decisions. A nearest neighbor criterion function is utilized as a means to minimize misclassification error between symbols. A development of the model to enhance class separability and legibility is shown in Figure 2 (Ref 17).

In this process, each symbol will be digitized into a pattern space so it can be processed by a computer. The discrete, two-dimensional Fourier transform will act as a feature selector. Low-pass filtering will be used to reduce the feature space of each symbol into a 49 component space. Euclidian distance between each transformed symbol will be used to determine the most confused symbols in each set. A symbol change algorithm will increase the distances between symbols as a means to increase separability between symbols. The inverse Fourier transform is performed and a spatial image is

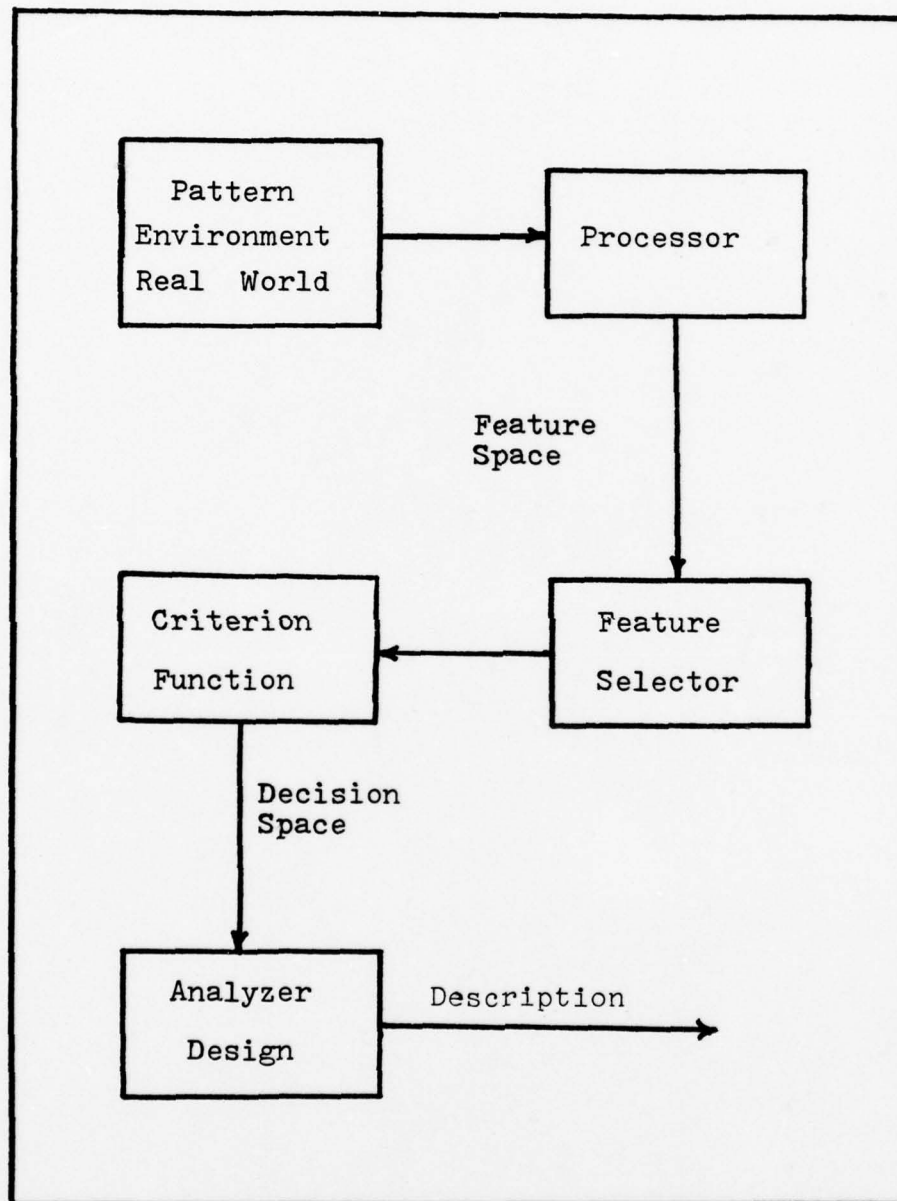


Figure 2. Development of Model

printed of the symbol being changed.

#### Input Symbol Representation

The Lincoln/Mitre, ASCII, Huddleston, and Namel, four fonts being tested by AFFDL, were digitized on a 14 unit high by 10 unit wide matrix grid. The IBM font was also included in this process. A Digital Equipment Corporation PDP-12 computer and a flying spot scanner are used to generate digitized symbols. All fonts were size normalized to the 10 X 14 grid. Each digitized symbol was punched onto computer cards by assigning an intensity of 1 or 0 to each grid of the input matrix. An example of the Lincoln/Mitre "A" is shown in Figure 3 below.

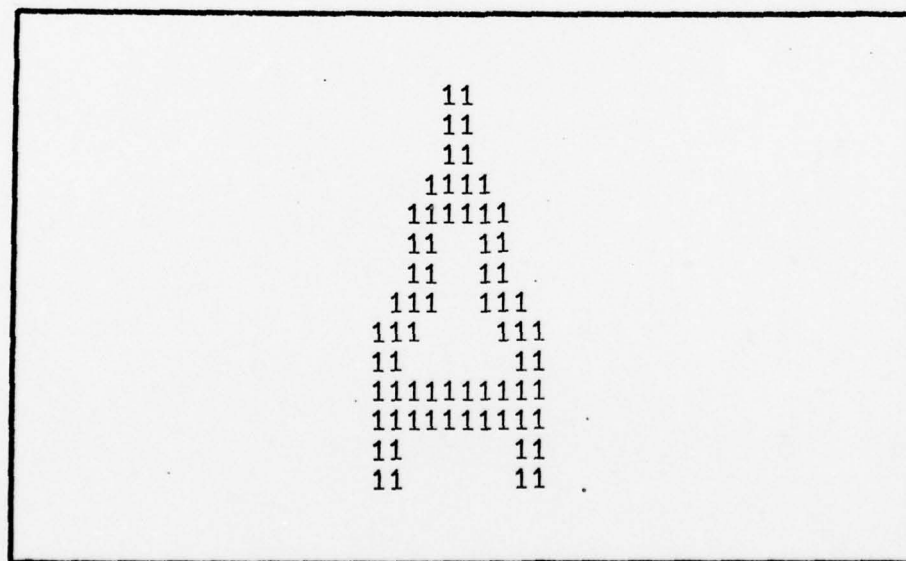


Figure 3. Lincoln/Mitre "A"

Each symbol is centered and imbedded in a zeroed 30 X 42 window array three times its size. The reason for this is to reduce edge effects, aliasing and leakage conditions that could occur due to the periodic nature of the Fourier transform. A test is made in Appendix F to determine what differences occur if symbols are used that fill the entire window. Figure 4 below shows the 30 X 42 input array of the letter "A" before computing its Fourier transform.

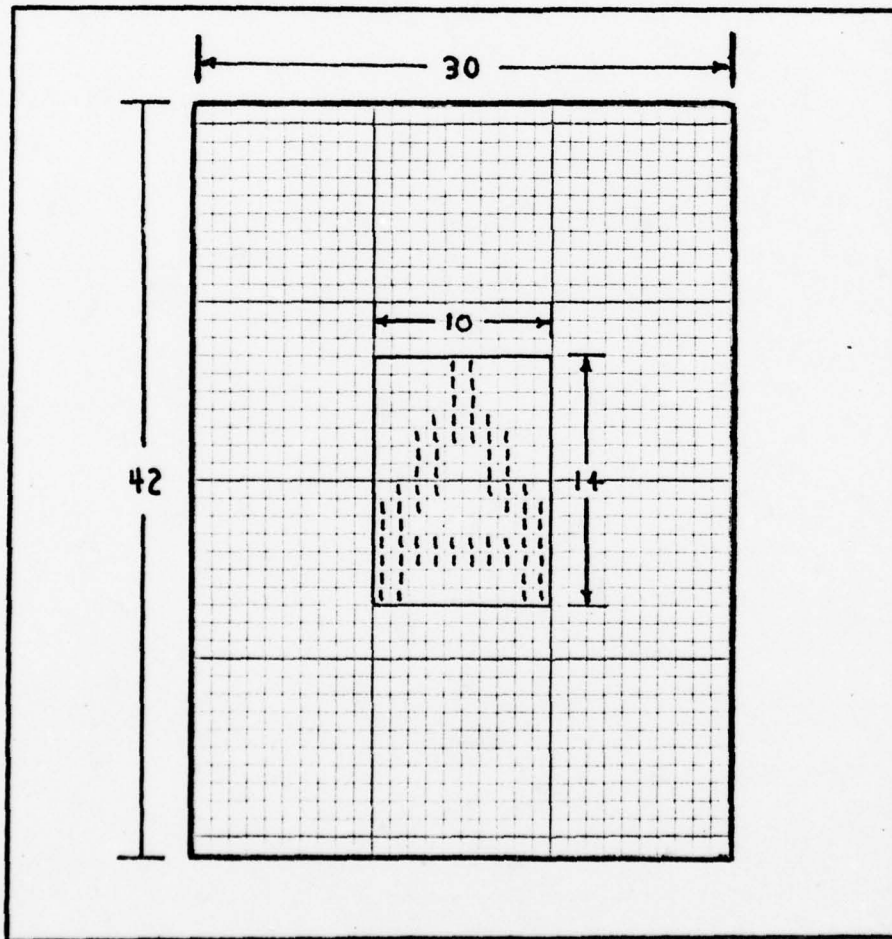


Figure 4. Window with Symbol Centered

## Fourier Analysis

There is a wide application of Fourier theory in electrical networks and communication systems. Recent development of the gas laser has also resulted in technical advances in Fourier optics. Fraunhofer diffraction patterns are discussed in Appendix D. In this thesis the Fourier transform is used as an analytical tool in two-dimensional image classification. Using present computer technology, the Fourier transform has adapted itself well to visual scene analysis.

The two-dimensional discrete Fourier transform is used to convert each symbol into its spatial frequency components. The inputted symbol represents the pattern space whose matrix size is in units of length. By means of the transform, the feature space represents the spectrum or spatial frequencies of the symbol. The Fourier transform may be considered as performing a spectral resolution of the pattern in which the corresponding phase and amplitude elements are obtained in a complex valued array (Ref 24:20,21).

The discrete, two-dimensional Fourier transform for a  $M \times N$  array  $X$  is:

$$F_{p,q} = \sum_{n=1}^N \sum_{m=1}^M X_{m,n} \exp -j2\pi \left[ (mp/M) + (nq/N) \right] \quad (1)$$

where  $X_{m,n}$  is a discrete point in the input pattern

space and  $F_{p,q}$  is the complex spatial frequency term in the feature space.

The Fourier transform is an orthogonal transform that preserves distance and angle between vectors. This transform changes the original array  $X$  into a set of Fourier coefficients that represent a system of sine and cosine functions which contain all the information of the original symbol. By using Euler's identity:

$$e^{\pm j\theta} = \cos\theta + j\sin\theta \quad (2)$$

equation (1) can be written as:

$$F_{p,q} = \sum_{n=1}^N \sum_{m=1}^M X_{m,n} \left[ \cos \frac{2\pi mp}{M} + \cos \frac{2\pi nq}{N} - j\sin \frac{2\pi mp}{M} - j\sin \frac{2\pi nq}{N} \right] \quad (3)$$

The inverse Fourier transform is:

$$X_{m,n} = \frac{1}{MN} \sum_{q=0}^{N-1} \sum_{p=0}^{M-1} F_{p,q} \exp j2\pi \left[ (mp/M) + (nq/N) \right] \quad (4)$$

By adding the correct Fourier components in the spatial frequency domain, the exact input pattern can be reproduced. Any visual pattern can be reconstructed from a finite sum of spatial sinusoids of appropriate spatial frequency, orientation, and amplitude. Like the Laplace transform, the Fourier transform is a linear operator with specific properties. Explanation and proof of the Fourier properties are found in Reference 12 and 24.

### Digital Computation

A Cooley-Tukey fast Fourier transform (Ref 5) is used in a subroutine called FOURT on the Control Data Corporation (CDC) 6600 computer to calculate each symbol's Fourier components. The zero frequency or DC term in the feature space (Fourier space) is located in the upper left corner of the real array. The DC term has a zero imaginary component. It is easier to locate the harmonics of the transformed frequencies by rearranging the FOURT matrix. Remember also that the imaginary part of each component is arranged in the same format. If the even 30 X 42 matrix (real and imaginary) is divided into four equal quadrants, the rearranged format is created by switching the first and fourth, and the second and third quadrants as shown in Figure 5.

Now the DC term will be located by the equation:

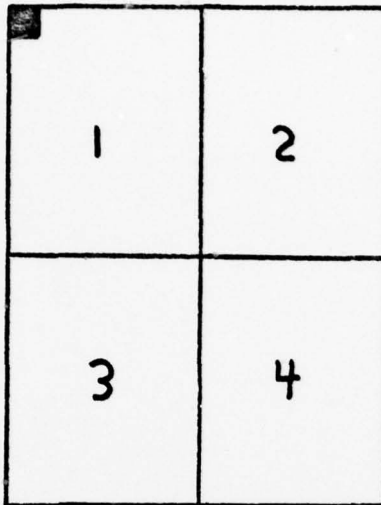
$$DC(p,q) = (M/2 + 1), (N/2 + 1) \quad (5)$$

The value of the DC term represents the total number of 1's in the inputted symbol. The first harmonic is the first ring of components surrounding the DC term and so forth for higher harmonics as shown in Figure 6. This method is used to identify the features that will be selected after filtering.

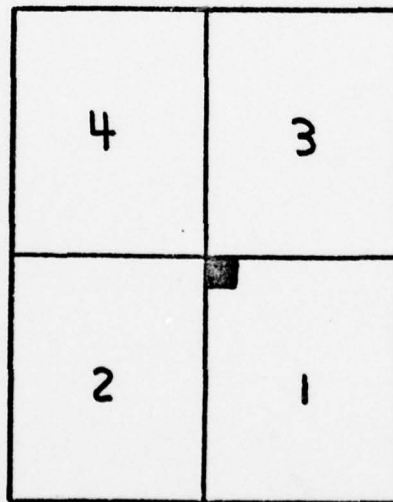
### Spatial Filtering

The number of features is reduced by spatial filtering. The application of the low pass filtering is

Fourier Array



Rearranged Fourier Array



■ DC Term

Figure 5. Rearranged Fourier Real Component Array

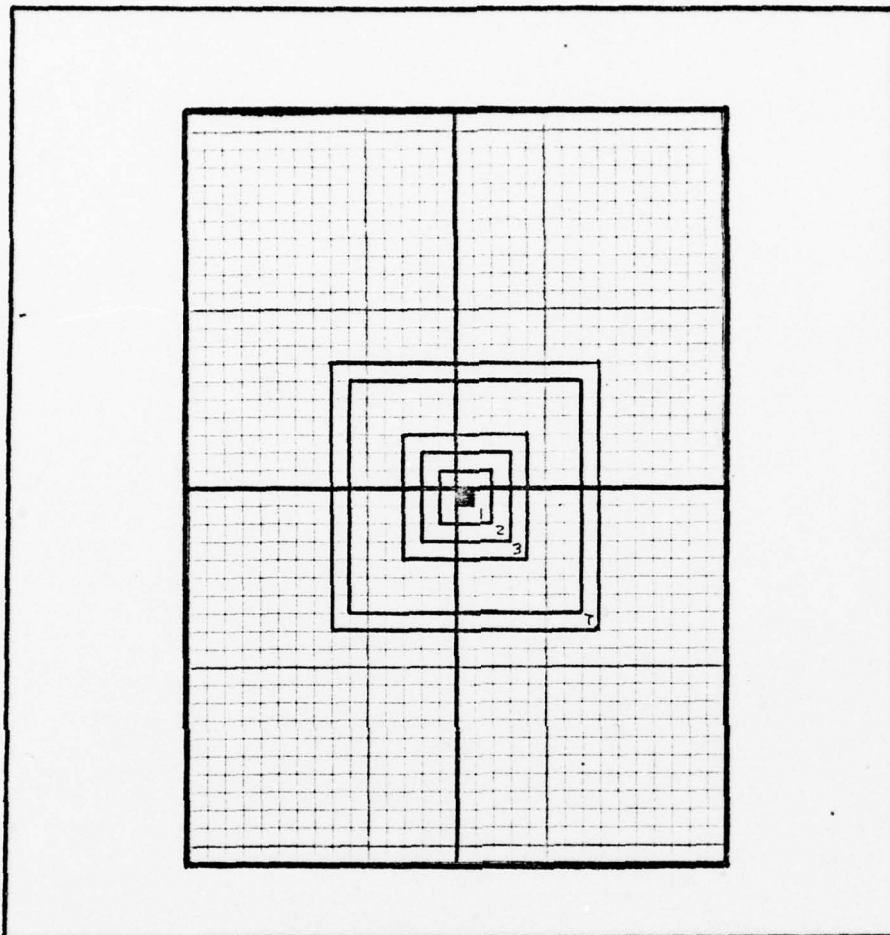


Figure 6. 1st, 2nd, 3rd, and 7th Harmonic of Window

based on the heuristic approach that has appeared reliable in symbol classification research in this area (Ref 3,4,20,24). One value of filtering is that it reduces computer computation time. The low spatial frequencies contain the majority of the energy or information of the original symbol. The fine detail or edge information is found in the higher spatial frequencies (Ref 7:309). A low-pass, 3rd harmonic filter of the

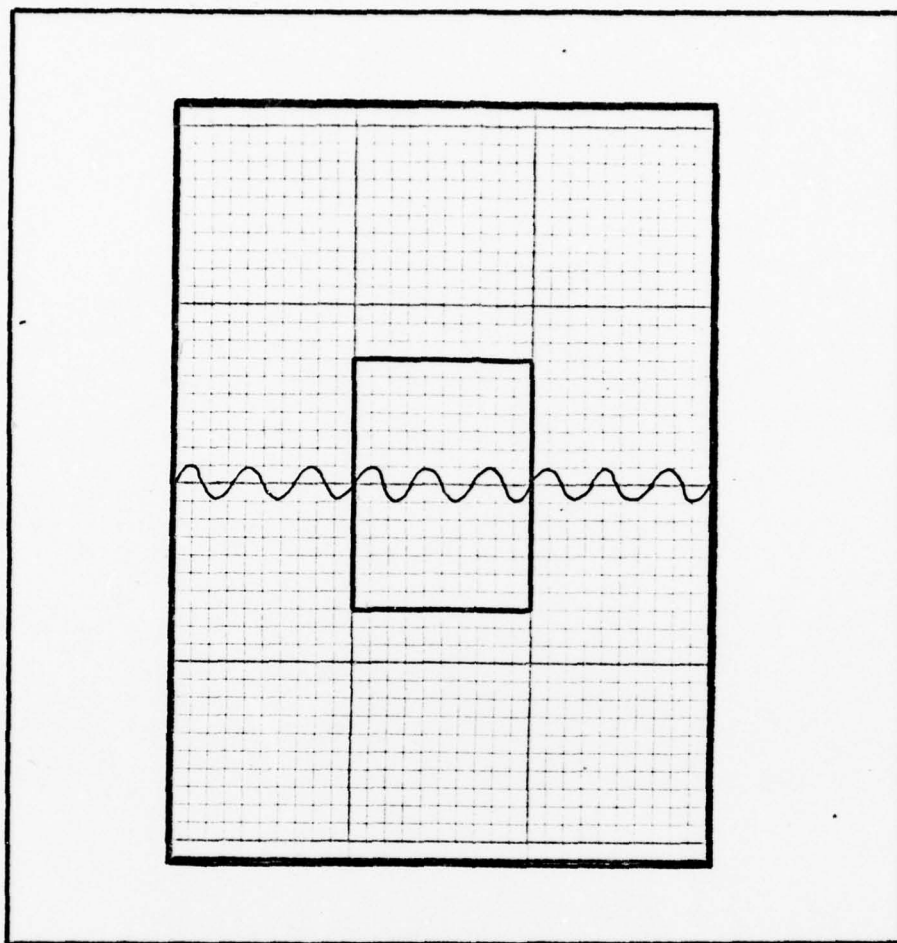


Figure 7. 9th Harmonic of Window

symbol was used. A 3rd harmonic filter of the symbol corresponds to the 9th harmonic of the window as shown in Figure 7 above. Every 3rd component in the first 9 rings around the DC term was kept as shown in the rearranged matrix and the FOURT Fourier component configuration in Figure 8. When the inverse transform is applied to this filtered array, 9 repeats of the symbol

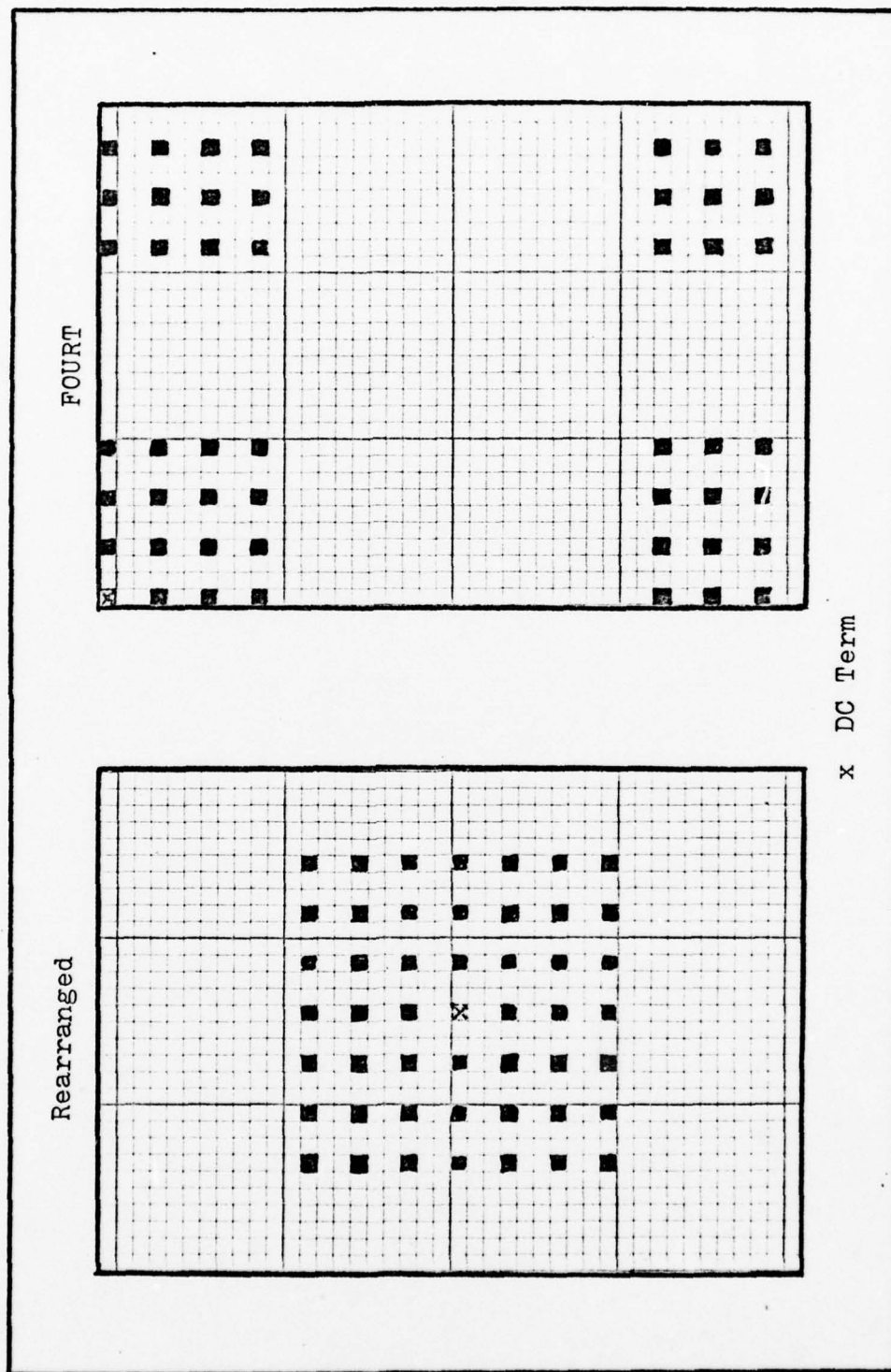


Figure 8. Rearranged and FOURT 3rd Harmonic Filter

occur as shown in Figure 9. This is due to the harmonic relationship between the window and the actual symbol. This is corrected to produce only one output prototype (Fig 10), by repacking the filtered components (Fig 11).

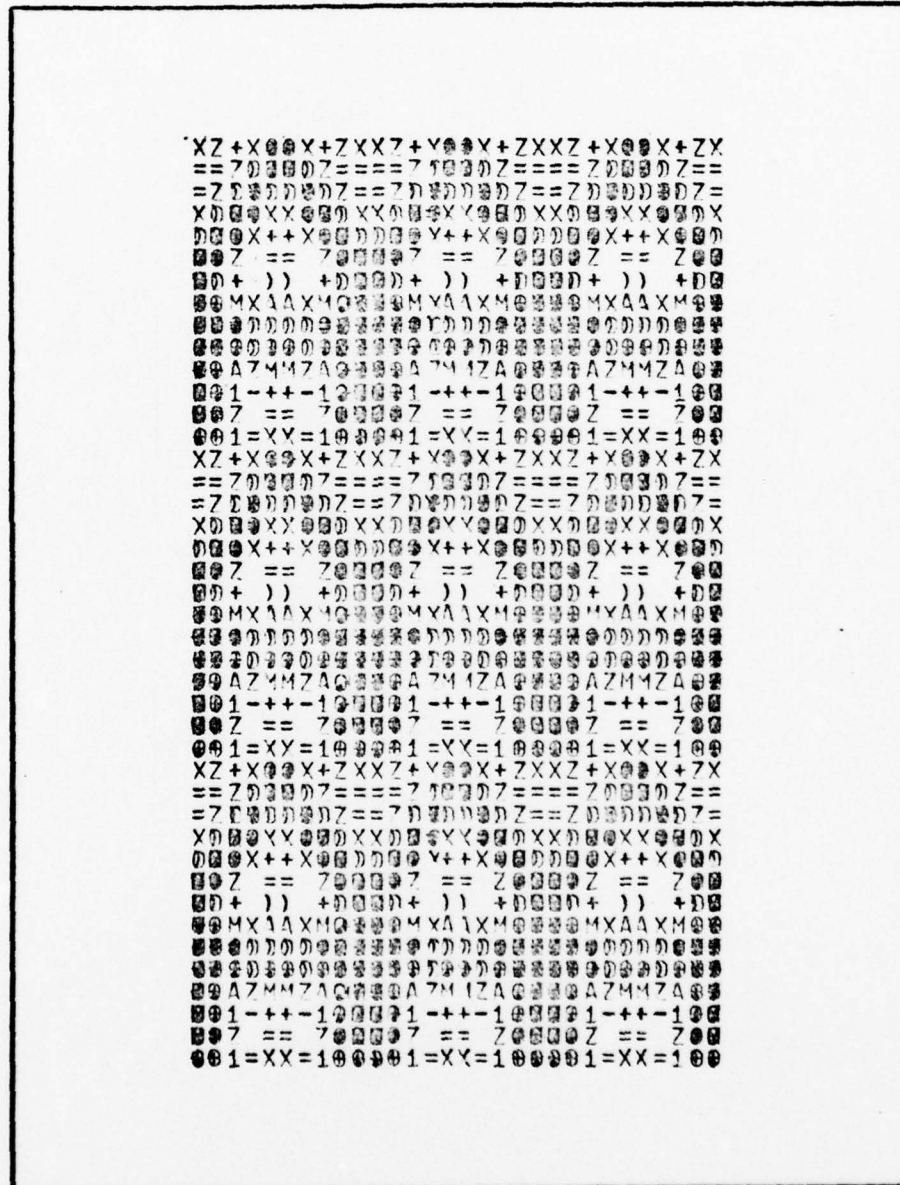


Figure 9. Reproduced Symbol with 9 Repeats

[illegible]

Figure 10. Reproduced Symbol Using Repacked Filter

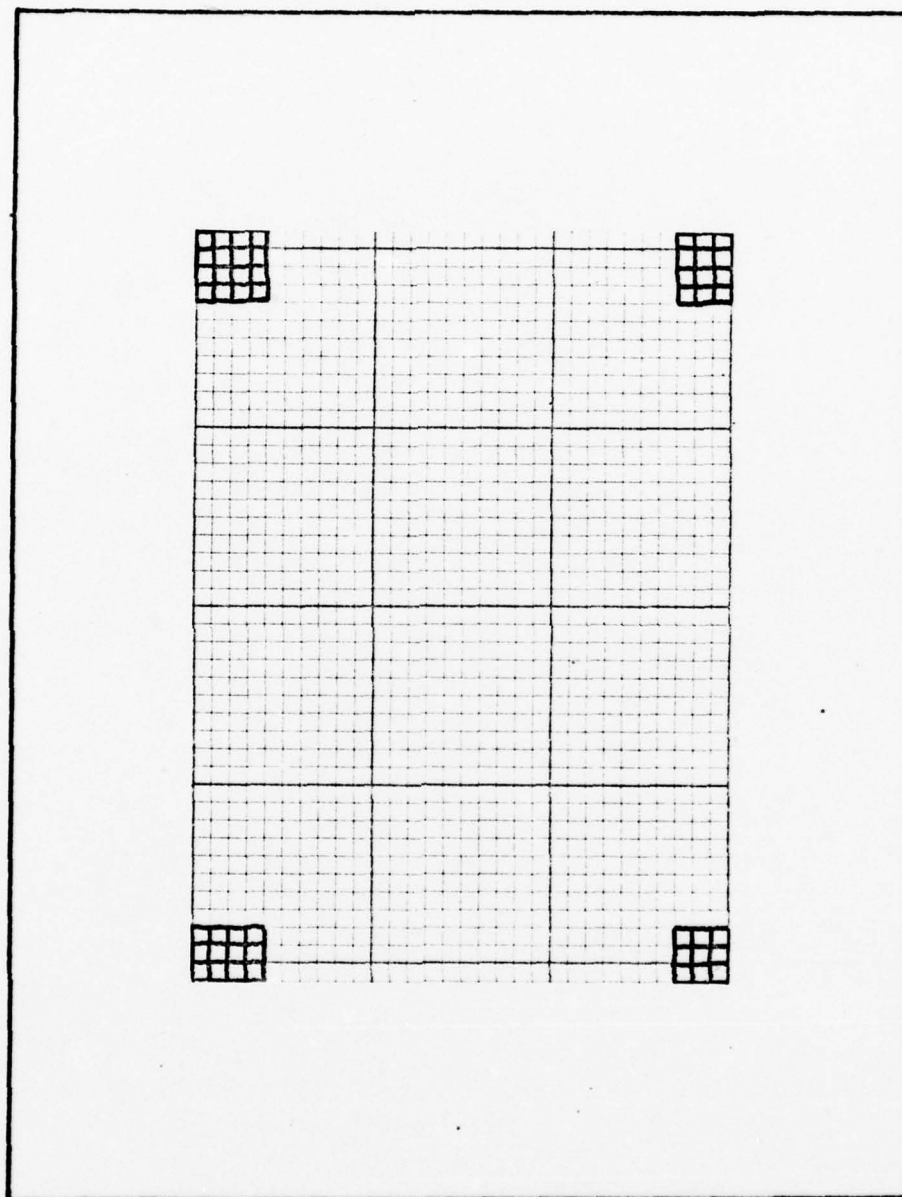


Figure 11. Repacked Filtered FOURT Array

-.763	-1.58	-.246	0.0	.246	1.58	.763
2.53	-2.15	-11.5	15.7	-11.5	-2.15	2.53
.357	4.49	6.89	0.0	-6.89	-4.49	-.357
6.91	9.85	18.1	64.0	18.1	9.85	6.91
-.357	-4.49	-6.89	0.0	6.89	4.49	.357
2.53	-2.15	-11.5	15.7	-11.5	-2.15	2.53
.763	1.58	.246	0.0	-.246	-1.58	-.763

Figure 12. Results after Filtering of L/M "P"

Due to the symmetry property of the Fourier transform, half of the features are identical. Figure 12 shows the real rearranged array with the Fourier components that were obtained from the Lincoln/Mitre (L/M) "P." The DC term equals 64, the number of 1's in the symbol "P." The line of symmetry separates the array into two identical parts, and is the same for the imaginary transformed array. The number of features needed can be reduced in half in which only the top 25 real and top 24 imaginary components are saved as shown in Figure 13. The imaginary part of the DC term is always zero. All other components are set to zero in the filter routine.

The DC feature is a measure of the average energy

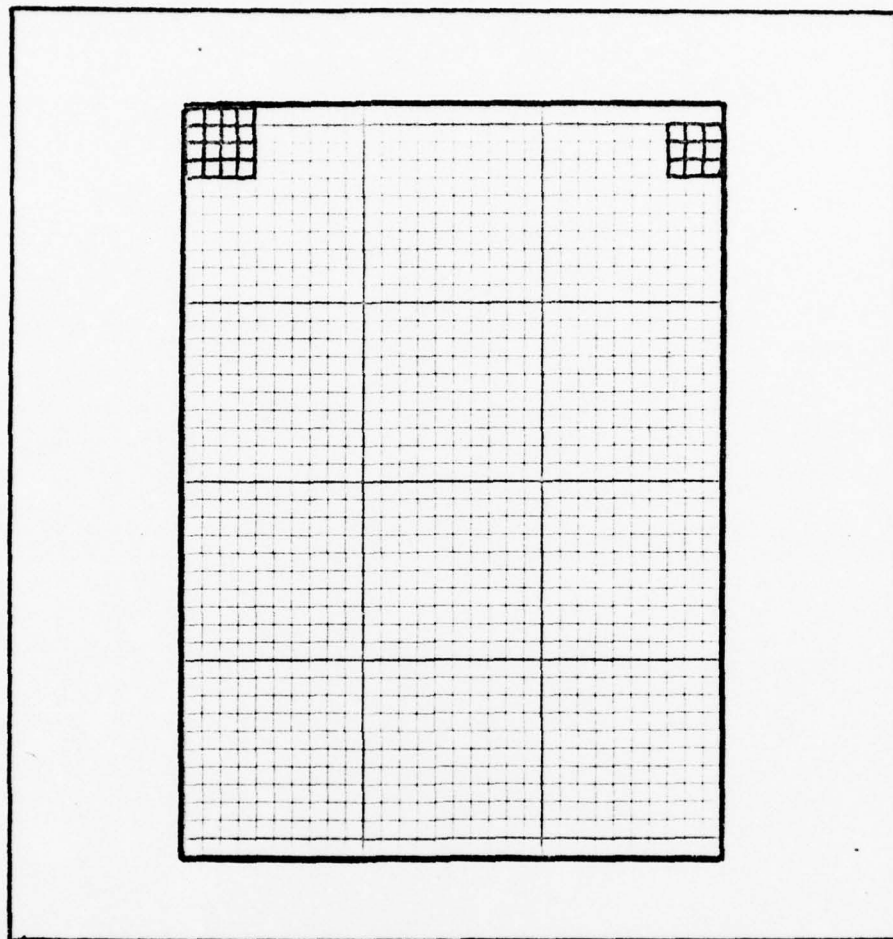


Figure 13. Fourier Real Array with 25 Components

of the symbol. Since each matrix dot is of the same intensity and different symbols contain varied numbers of charged LED's, there is different intensity levels between symbols. The DC term was set to zero in the filter due to the insignificance of intensity in symbol identification in the human visual system (Ref 13:317) and (Ref 14:47).

Campbell and Robson (Ref 2:551-556) measured the contrast thresholds of a variety of grating patterns over a wide range of spatial frequencies. They obtained curves for  $2^\circ$  and for  $10^\circ$  fields of view with viewing distances of 285 cm and 57 cm as shown in Figure 14.

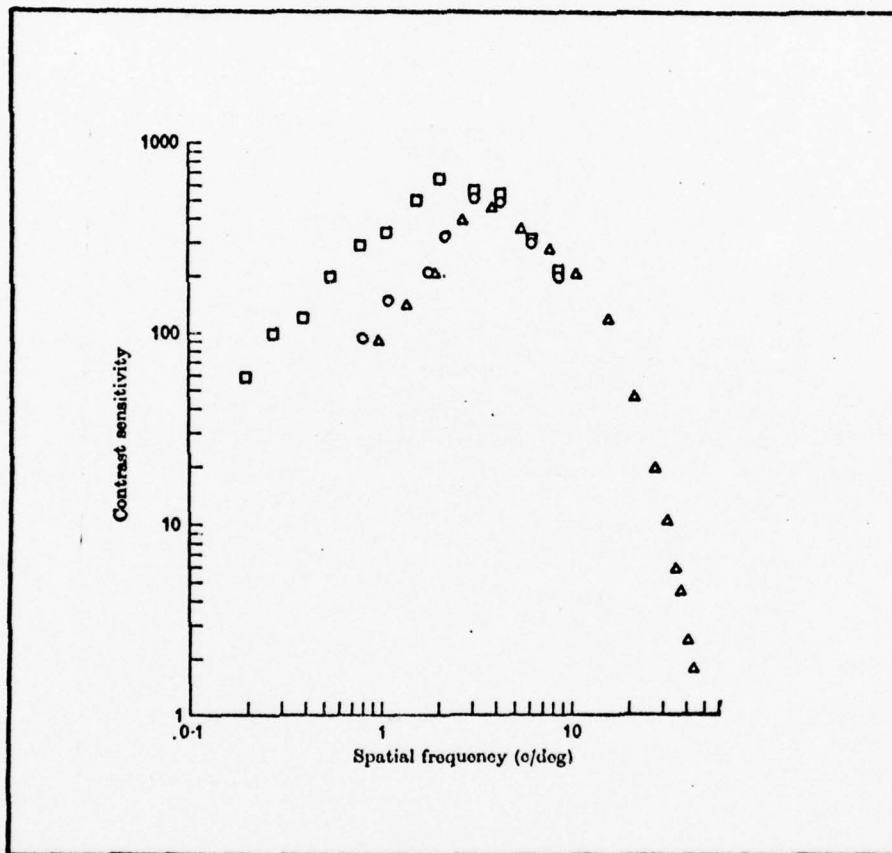


Figure 14. Contrast sensitivity for sine-wave gratings. Luminance  $500 \text{ cd/m}^2$ . Viewing distance 285 cm and aperture  $2^\circ \times 2^\circ$ ,  $\Delta$ ; viewing distance 57 cm, aperture  $10^\circ \times 10^\circ$ ,  $\square$ ; viewing distance 57 cm, aperture  $2^\circ \times 2^\circ$ ,  $\circ$ . (From Ref 2:554)

The low spatial frequencies show small contrast sensi-

tivity with the valve increasing to a peak at approximately 3 cycles/degree. This is shown in Figure 3 where the zero cycles/degree (DC) has insignificant contrast. Gagnon (Ref 9) shows similar results using the modulation transfer function (MTF). The human MTF normally shows the spatial frequency response of the eye to have a peak sensitive from 5 cycles/degree to 12 cycles/degree, depending on the brightness, and lower frequencies attenuated for monochromatic, foveal stimuli.

#### Energy Normalization

The filtered array  $X$  is energy normalized by the equation:

$$\bar{X}_{i,j} = X_{i,j} \left[ \sum_{i=1}^{30} \sum_{j=1}^{42} |X_{i,j}|^2 \right]^{-\frac{1}{2}}$$

where  $\bar{X}_{i,j}$  is the normalized  $ij$ th element. Each symbol is made up of the 49 features. The 49 Fourier components can define a vector or point in 49 space. When normalized, the point representing each symbol will fall on a hypersphere of radius 1. The distance between symbols will be chords on this sphere. The maximum distance being two. After normalization, the total energy in  $\bar{X}$  is equal to unity.

A normalized function is identical to the same function with a gain constant multiple. This is shown

below where the Fourier transform of the function  $a_n$  is:

$$a_n \longleftrightarrow A_p \quad (6)$$

and after  $A_p$  is energy normalized it is represented by:

$$\frac{A_p}{\sqrt{\sum_{n=1}^N a_n^2}} \quad (7)$$

Now if  $a_n$  has a gain,  $k$  where  $b_n = ka_n$ , the Fourier transform is:

$$ka_n \longleftrightarrow kA_p = B_p \quad (8)$$

and after it is energy normalized:

$$\frac{B_p}{\sqrt{\sum_{n=1}^N b_n^2}} = \frac{kA_p}{k\sqrt{\sum_{n=1}^N a_n^2}} = \frac{A_p}{\sqrt{\sum_{n=1}^N a_n^2}} \quad (9)$$

Equation (7) and (9) are the same. This shows how normalization can equate symbols with gain differences. This could be caused by a varied intensity of the charged light-emitted diodes.

Energy normalization is performed after filtering to insure that the points for each prototype fall on the unit hypersphere. Energy normalization prior to filtering will cause the points to move off the hypersphere once filtering takes place.

#### Euclidian Distance

The 49 energy normalized Fourier components can now represent features of each symbol. Each 36 symbol

alphanumeric font can be plotted as 36 points on a hypersphere. Similar symbols may cluster together on the hypersphere. It is these symbols that are close together in the Euclidian distance sense that are likely to be more confused than those that are far apart. The Euclidian distance between each vector or symbol on the hypersphere is calculated. The symbols and their distances can be compared to their human error data. If A and B are the position vectors of two symbols in the feature space and the distance between A and B is:

$$\text{Dist}_{AB} = |A-B| \quad (10)$$

and the Euclidian distance for 49 component vectors is

$$\text{Dist}_{AB} = \sqrt{\sum_{i=1}^{49} (A_i - B_i)^2} \quad (11)$$

where  $A_i$  and  $B_i$  are the  $i^{\text{th}}$  component of each vector.

A distance matrix between all symbols in a set is printed out. Table I and Table II are the Euclidian distance matrix for the Lincoln/Mitre font. The value on one side of the diagonal of the matrix are identical to those on the other side. This is due to the fact that the distance from "A" to "B" is the same as from "B" to "A". The diagonal elements are zero since the distance from each symbol to itself is zero. The statistical mean and the standard deviation are also

Table I  
Lincoln/Mitre Distance Matrix A - R

	A	B	C	AGAINST	E	F	G	H	I	J	K	L	M	N	O	P	Q	R
LINCOLN/MITRE					THEMSELVES													
A	0.0000	1.4737	1.4926	1.3842	1.5693	1.5306	1.4811	1.4098	1.6787	1.4262	1.4098	1.4773	1.4634	1.5062	1.5085	1.5801	1.7137	1.5464
B	1.4737	0.0000	1.4412	0.9751	1.3776	1.4536	1.6382	1.4400	1.2676	1.1955	1.7637	1.5589	1.5919	1.5053	1.2865	1.3386	1.4500	1.4580
C	1.4926	1.4412	0.0000	1.5160	1.1337	1.3090	1.3164	1.4921	1.3075	1.3785	1.4701	1.1347	1.8225	1.3326	1.1967	1.4085	1.4100	1.4563
D	1.3842	0.9751	1.5160	0.0000	1.5426	1.5605	1.3505	1.5029	1.4397	1.2731	1.6554	1.5588	1.5359	1.5532	1.4023	1.5328	1.5040	1.6048
E	1.5693	1.3776	1.1337	1.5426	0.0000	0.5255	1.2513	1.0849	1.2066	1.4624	1.2565	0.8224	1.3903	1.3360	1.0929	0.9282	1.3374	1.0419
F	1.5306	1.4536	1.3090	1.5605	0.5255	0.0000	1.2838	0.9585	1.4062	1.5928	1.1755	1.1169	1.2820	1.2654	1.2107	0.6251	1.2664	0.8945
G	1.4811	1.6382	1.3164	1.3505	1.2513	1.2838	0.0000	1.5031	1.2842	1.3590	1.3068	1.1210	1.4500	1.4340	1.0767	1.3357	1.2897	1.3041
H	1.4098	1.4400	1.4921	1.5029	1.0849	0.9585	1.5031	0.0000	1.7049	1.4885	1.1733	1.1482	0.9084	0.8933	1.1924	0.9540	1.2972	1.0326
I	1.6787	1.2676	1.3075	1.4397	1.2066	1.4062	1.2842	1.7049	0.0000	1.3904	1.5374	1.4049	1.6942	1.5875	1.2792	1.4319	1.3554	1.4165
J	1.4262	1.1955	1.3785	1.2731	1.4624	1.5928	1.3590	1.4885	1.3904	0.0000	1.5796	1.4432	1.5015	1.5255	1.1927	1.5116	1.4557	1.5240
K	1.4098	1.7637	1.4701	1.6554	1.2565	1.1755	1.3068	1.1733	1.5374	1.5796	0.0000	1.1203	1.1200	1.1088	1.5159	1.2569	1.3351	1.0305
L	1.4773	1.5588	1.1347	1.5588	0.8224	1.1169	1.1210	1.1482	1.4043	1.4432	1.1203	0.0000	1.2063	1.2052	1.0965	1.1912	1.4830	1.2059
M	1.4634	1.5919	1.4225	1.5359	1.3903	1.2820	1.4500	0.9034	1.6942	1.5015	1.1200	1.2063	0.0000	0.9652	1.1865	1.2610	1.4153	1.3579
N	1.5062	1.5053	1.4326	1.5532	1.3360	1.2664	1.4340	0.8933	1.5875	1.5255	1.1088	1.2032	0.9652	0.0000	1.2470	1.2794	1.2272	1.1273
O	1.6085	1.2895	1.1967	1.4023	1.0929	1.2107	1.0767	1.1924	1.2792	1.1927	1.5159	1.0965	1.1866	1.2470	0.0000	1.1254	1.2140	1.2457
P	1.5801	1.3386	1.4085	1.5328	0.9262	0.5251	1.3367	0.9540	1.4319	1.5116	1.2569	1.1912	1.2610	1.2794	1.1254	0.0000	1.1955	0.5770
Q	1.7137	1.4500	1.4100	1.5048	1.3374	1.2664	1.2897	1.2972	1.3554	1.4557	1.3351	1.4830	1.4533	1.2272	1.2140	1.1955	0.0000	0.9470
R	1.5464	1.4580	1.4563	1.6048	1.0419	0.8945	1.3081	1.0326	1.4165	1.5240	1.0305	1.2059	1.3579	1.1273	1.2457	0.6730	0.9470	0.0000
S	1.4749	1.2821	1.3341	1.3101	1.4055	1.4684	1.1675	1.5932	1.2116	1.3181	1.5155	1.4174	1.6008	1.4705	1.3235	1.4942	1.4520	1.5180
T	1.5927	1.4546	1.3563	1.5098	1.3155	1.1162	1.4123	1.6034	0.8600	1.5506	1.4076	1.5165	1.4174	1.5476	1.5119	1.3955	1.4088	1.3293
U	1.5654	1.4431	1.2963	1.4854	1.1346	1.2646	1.2532	0.9032	1.2000	1.3561	0.9239	1.0034	1.0163	0.7098	1.2484	1.3876	1.3055	1.3935
V	1.5592	1.3042	1.4319	1.3186	1.4054	1.7855	1.4631	1.2869	1.6700	1.2151	1.4214	1.4084	1.5201	1.4602	1.4686	1.2840	1.2269	1.3005
W	1.6582	1.4478	1.4318	1.4617	1.3711	1.3540	1.4202	1.3354	1.3669	1.3759	1.3320	1.4088	1.4713	1.3857	1.4011	1.3494	1.0765	1.3545
X	1.5761	1.4199	1.5099	1.5497	1.4742	1.3873	1.3309	1.1734	1.6266	1.4829	1.2129	1.4128	1.3039	1.1937	1.6412	1.3518	1.4534	1.3144
Y	1.5761	1.4732	1.5230	1.5373	1.4788	1.4401	1.5559	1.3733	1.3675	1.4861	1.3213	1.4686	1.4379	1.2922	1.6017	1.3774	1.4783	1.3911
Z	1.5493	1.457	1.3484	1.4028	0.9008	1.0874	1.5453	1.2777	1.1951	1.3211	1.4406	1.2448	1.5247	1.5235	1.3194	1.1188	1.3773	1.1974
0	1.5659	1.5554	1.4417	1.4730	1.5988	1.4460	1.5086	1.4013	1.5195	1.4568	1.3052	1.5724	1.2361	1.3994	1.5910	1.4470	1.2724	1.5017
1	1.4002	1.5530	1.4199	1.5310	1.4890	1.5089	1.3762	1.6237	0.9641	1.5350	1.4343	1.5303	1.6049	1.5690	1.5663	1.5295	1.4480	1.4878
2	1.4540	1.1978	1.7882	1.2980	1.4198	1.4461	1.3647	1.5271	1.2625	1.2217	1.5000	1.4194	1.5341	1.5348	1.3018	1.3172	1.4496	1.3391
3	1.4074	1.1928	1.4280	1.4054	1.2356	1.3828	1.3384	1.4954	1.0908	1.1306	1.5051	1.3817	1.3622	1.6195	1.4873	1.4562	1.6060	1.5473
4	1.2485	1.5454	1.1972	1.5476	1.4626	1.4163	1.1705	1.5716	1.5173	1.2983	1.4303	1.3622	1.4775	1.4717	1.3319	1.4064	1.4408	1.3930
5	1.5805	1.1939	1.2165	1.4816	0.8462	1.0021	1.2366	1.1975	1.1818	1.4030	1.4117	1.0463	1.4544	1.3875	1.0949	1.1601	1.2963	1.2368
6	1.2805	1.3175	1.3920	1.3594	1.4283	1.5028	1.3749	1.5545	1.2767	1.0828	1.4081	1.4832	1.6032	1.6266	1.4993	1.5365	1.5610	1.5891
7	1.5919	1.3218	1.4220	1.4834	1.3556	1.3544	1.4345	1.5250	1.1860	1.3546	1.5515	1.5469	1.5937	1.5960	1.4591	1.2669	1.3747	1.2778
8	1.3924	1.6559	1.3802	1.4098	1.0854	1.1937	1.2715	1.2378	1.2081	1.2298	1.5200	1.2667	1.4769	1.3963	1.0987	1.1757	1.5284	1.3415
9	1.5001	1.2130	1.4463	1.3066	1.4353	1.3451	1.3987	1.5545	1.2767	1.3591	1.5760	1.6417	1.6697	1.5853	1.4983	1.2563	1.3263	1.3037

Table II

MEAN= 1.3706 STANDARD DEVIATION= .1766

calculated. They are printed below the distance matrix.

All the distances are then sorted from smallest to largest. Table III shows the sorted A-L for the Lincoln/Mitre set; Table IV shows M-X, while Table V shows Y-9.

A histogram of the Euclidian distance data for the Lincoln/Mitre font is shown in Figure 15. The distance range between 0 and 2 was divided into 40 bins or .05 units for each subdivision on the distance axis. For example, bin 20 represents distances greater than .95 and less than or equal to 1.00. Note for a 36 symbol font there are always 36 values in bin 1 due to zero distance for like symbols. The distance histogram shows a gaussian distribution of the data.

#### Symbol Rating

Using Euclidian distance as a decision rule, each font can be rank ordered by the distance between each symbol and its nearest neighbor. The symbol pair with the shortest distance is ranked first in being a confusing symbol. All pairs are ranked until the last pair is the one with the greatest distance between prototype and nearest neighbor as shown in Table VI. Now the 3rd column is checked for each pair in order to rank the two symbols in the pair. A rank order of the

Table III  
Lincoln/Mitre Sorted Distance Matrix A - L

LINCOLN/MITRE		AGAINST THEMSELVES		10/07/77		14.06.06.		FILTERED 7 x 7	
A	S	A	S	A	S	A	S	A	S
A	0.000	1.337	1.134	1.009	1.192	1.002	1.409	1.426	1.450
B	1.337	0.000	1.337	1.134	1.009	1.402	1.426	1.450	1.473
C	1.134	1.337	0.000	1.337	1.134	1.002	1.409	1.426	1.450
D	1.009	1.192	1.402	1.426	1.450	1.473	1.496	1.519	1.542
E	1.192	1.402	1.426	1.450	1.473	1.496	1.519	1.542	1.565
F	1.402	1.426	1.450	1.473	1.496	1.519	1.542	1.565	1.588
G	1.426	1.450	1.473	1.496	1.519	1.542	1.565	1.588	1.611
H	1.450	1.473	1.496	1.519	1.542	1.565	1.588	1.611	1.634
I	1.473	1.496	1.519	1.542	1.565	1.588	1.611	1.634	1.657
J	1.496	1.519	1.542	1.565	1.588	1.611	1.634	1.657	1.680
K	1.519	1.542	1.565	1.588	1.611	1.634	1.657	1.680	1.703
L	1.542	1.565	1.588	1.611	1.634	1.657	1.680	1.703	1.726
M	1.565	1.588	1.611	1.634	1.657	1.680	1.703	1.726	1.749
N	1.588	1.611	1.634	1.657	1.680	1.703	1.726	1.749	1.772
O	1.611	1.634	1.657	1.680	1.703	1.726	1.749	1.772	1.795
P	1.634	1.657	1.680	1.703	1.726	1.749	1.772	1.795	1.818
Q	1.657	1.680	1.703	1.726	1.749	1.772	1.795	1.818	1.841
R	1.680	1.703	1.726	1.749	1.772	1.795	1.818	1.841	1.864
S	1.703	1.726	1.749	1.772	1.795	1.818	1.841	1.864	1.887
T	1.726	1.749	1.772	1.795	1.818	1.841	1.864	1.887	1.910
U	1.749	1.772	1.795	1.818	1.841	1.864	1.887	1.910	1.933
V	1.772	1.795	1.818	1.841	1.864	1.887	1.910	1.933	1.956
W	1.795	1.818	1.841	1.864	1.887	1.910	1.933	1.956	1.979
X	1.818	1.841	1.864	1.887	1.910	1.933	1.956	1.979	2.002
Y	1.841	1.864	1.887	1.910	1.933	1.956	1.979	2.002	2.025
Z	1.864	1.887	1.910	1.933	1.956	1.979	2.002	2.025	2.048
AA	1.887	1.910	1.933	1.956	1.979	2.002	2.025	2.048	2.071
AB	1.910	1.933	1.956	1.979	2.002	2.025	2.048	2.071	2.094
AC	1.933	1.956	1.979	2.002	2.025	2.048	2.071	2.094	2.117
AD	1.956	1.979	2.002	2.025	2.048	2.071	2.094	2.117	2.140
AE	1.979	2.002	2.025	2.048	2.071	2.094	2.117	2.140	2.163
AF	2.002	2.025	2.048	2.071	2.094	2.117	2.140	2.163	2.186
AG	2.025	2.048	2.071	2.094	2.117	2.140	2.163	2.186	2.209
AH	2.048	2.071	2.094	2.117	2.140	2.163	2.186	2.209	2.232
AI	2.071	2.094	2.117	2.140	2.163	2.186	2.209	2.232	2.255
AJ	2.094	2.117	2.140	2.163	2.186	2.209	2.232	2.255	2.278
AK	2.117	2.140	2.163	2.186	2.209	2.232	2.255	2.278	2.301
AL	2.140	2.163	2.186	2.209	2.232	2.255	2.278	2.301	2.324
AM	2.163	2.186	2.209	2.232	2.255	2.278	2.301	2.324	2.347
AN	2.186	2.209	2.232	2.255	2.278	2.301	2.324	2.347	2.370
AO	2.209	2.232	2.255	2.278	2.301	2.324	2.347	2.370	2.393
AP	2.232	2.255	2.278	2.301	2.324	2.347	2.370	2.393	2.416
AQ	2.255	2.278	2.301	2.324	2.347	2.370	2.393	2.416	2.439
AR	2.278	2.301	2.324	2.347	2.370	2.393	2.416	2.439	2.462
AS	2.301	2.324	2.347	2.370	2.393	2.416	2.439	2.462	2.485
AT	2.324	2.347	2.370	2.393	2.416	2.439	2.462	2.485	2.508
AU	2.347	2.370	2.393	2.416	2.439	2.462	2.485	2.508	2.531
AV	2.370	2.393	2.416	2.439	2.462	2.485	2.508	2.531	2.554
AW	2.393	2.416	2.439	2.462	2.485	2.508	2.531	2.554	2.577
AX	2.416	2.439	2.462	2.485	2.508	2.531	2.554	2.577	2.600
AY	2.439	2.462	2.485	2.508	2.531	2.554	2.577	2.600	2.623
AZ	2.462	2.485	2.508	2.531	2.554	2.577	2.600	2.623	2.646
BA	2.485	2.508	2.531	2.554	2.577	2.600	2.623	2.646	2.669
BB	2.508	2.531	2.554	2.577	2.600	2.623	2.646	2.669	2.692
BC	2.531	2.554	2.577	2.600	2.623	2.646	2.669	2.692	2.715
BD	2.554	2.577	2.600	2.623	2.646	2.669	2.692	2.715	2.738
BE	2.577	2.600	2.623	2.646	2.669	2.692	2.715	2.738	2.761
BF	2.600	2.623	2.646	2.669	2.692	2.715	2.738	2.761	2.784
BG	2.623	2.646	2.669	2.692	2.715	2.738	2.761	2.784	2.807
BH	2.646	2.669	2.692	2.715	2.738	2.761	2.784	2.807	2.830
BI	2.669	2.692	2.715	2.738	2.761	2.784	2.807	2.830	2.853
BJ	2.692	2.715	2.738	2.761	2.784	2.807	2.830	2.853	2.876
BK	2.715	2.738	2.761	2.784	2.807	2.830	2.853	2.876	2.899
BL	2.738	2.761	2.784	2.807	2.830	2.853	2.876	2.899	2.922
BM	2.761	2.784	2.807	2.830	2.853	2.876	2.899	2.922	2.945
BN	2.784	2.807	2.830	2.853	2.876	2.899	2.922	2.945	2.968
BO	2.807	2.830	2.853	2.876	2.899	2.922	2.945	2.968	2.991
BP	2.830	2.853	2.876	2.899	2.922	2.945	2.968	2.991	3.014
BQ	2.853	2.876	2.899	2.922	2.945	2.968	2.991	3.014	3.037
BR	2.876	2.899	2.922	2.945	2.968	2.991	3.014	3.037	3.060
BS	2.899	2.922	2.945	2.968	2.991	3.014	3.037	3.060	3.083
BT	2.922	2.945	2.968	2.991	3.014	3.037	3.060	3.083	3.106
BU	2.945	2.968	2.991	3.014	3.037	3.060	3.083	3.106	3.129
BV	2.968	2.991	3.014	3.037	3.060	3.083	3.106	3.129	3.152
BW	2.991	3.014	3.037	3.060	3.083	3.106	3.129	3.152	3.175
BX	3.014	3.037	3.060	3.083	3.106	3.129	3.152	3.175	3.198
BY	3.037	3.060	3.083	3.106	3.129	3.152	3.175	3.198	3.221
BZ	3.060	3.083	3.106	3.129	3.152	3.175	3.198	3.221	3.244
CA	3.083	3.106	3.129	3.152	3.175	3.198	3.221	3.244	3.267
CB	3.106	3.129	3.152	3.175	3.198	3.221	3.244	3.267	3.290
CC	3.129	3.152	3.175	3.198	3.221	3.244	3.267	3.290	3.313
CD	3.152	3.175	3.198	3.221	3.244	3.267	3.290	3.313	3.336
CE	3.175	3.198	3.221	3.244	3.267	3.290	3.313	3.336	3.359
CF	3.198	3.221	3.244	3.267	3.290	3.313	3.336	3.359	3.382
CG	3.221	3.244	3.267	3.290	3.313	3.336	3.359	3.382	3.405
CH	3.244	3.267	3.290	3.313	3.336	3.359	3.382	3.405	3.428
CI	3.267	3.290	3.313	3.336	3.359	3.382	3.405	3.428	3.451
CJ	3.290	3.313	3.336	3.359	3.382	3.405	3.428	3.451	3.474
CK	3.313	3.336	3.359	3.382	3.405	3.428	3.451	3.474	3.497
CL	3.336	3.359	3.382	3.405	3.428	3.451	3.474	3.497	3.520
CM	3.359	3.382	3.405	3.428	3.451	3.474	3.497	3.520	3.543
CN	3.382	3.405	3.428	3.451	3.474	3.497	3.520	3.543	3.566
CO	3.405	3.428	3.451	3.474	3.497	3.520	3.543	3.566	3.589
CP	3.428	3.451	3.474	3.497	3.520	3.543	3.566	3.589	3.612
CQ	3.451	3.474	3.497	3.520	3.543	3.566	3.589	3.612	3.635
CR	3.474	3.497	3.520	3.543	3.566	3.589	3.612	3.635	3.658
CS	3.497	3.520	3.543	3.566	3.589	3.612	3.635	3.658	3.681
CT	3.520	3.543	3.566	3.589	3.612	3.635	3.658	3.681	3.704
CU	3.543	3.566	3.589	3.612	3.635	3.658	3.681	3.704	3.727
CV	3.566	3.589	3.612	3.635	3.658	3.681	3.704	3.727	3.750
CW	3.589	3.612	3.635	3.658	3.681	3.704	3.727	3.750	3.773
CX	3.612	3.635	3.658	3.681	3.704	3.727	3.750	3.773	3.796
CY	3.635	3.658	3.681	3.704	3.727	3.750	3.773	3.796	3.819
CZ	3.658	3.681	3.704	3.727	3.750	3.773	3.796	3.819	3.842
DA	3.681	3.704	3.727	3.750	3.773	3.796	3.819	3.842	3.865
DB	3.704	3.727	3.750	3.773	3.796	3.819	3.842	3.865	3.888
DC	3.727	3.750	3.773	3.796	3.819	3.842	3.865	3.888	3.911
DD	3.750	3.773	3.796	3.819	3.842	3.865	3.888	3.911	3.934
DE	3.773	3.796	3.819	3.842	3.865	3.888	3.911	3.934	3.957
DF	3.796	3.819	3.842	3.865	3.888	3.911	3.934	3.957	3.980
DG	3.819	3.842	3.865	3.888	3.911	3.934	3.957	3.980	4.003
DH	3.842	3.865	3.888	3.911	3.934	3.957	3.980	4.003	4.026
DI	3.865	3.888	3.911	3.934	3.957	3.980	4.003	4.026	4.049
DJ	3.888	3.911	3.934	3.957	3.980	4.003	4.026	4.049	4.072
DK	3.911	3.934	3.957	3.980	4.003	4.026	4.049	4.072	4.095
DL	3.934	3.957	3.980	4.003	4.026	4.049	4.072	4.095	4.118
DM	3.957	3.980	4.003	4.026	4.049	4.072	4.095	4.118	4.141
DN	3.980	4.003	4.026	4.049	4.072	4.095	4.118	4.141	4.164
DO	4.003	4.026	4.049	4.072	4.095	4.118	4.141		

Table IV  
Lincoln/Mitre Sorted Distance Matrix M - X

LINCOLN/PATR		AGAINST THEMSELVES		10/03/77		14.04.06.		FILTERED 7 x 7										
M	0.0000	0.254	0.9552	1.004	1.200	1.0666	1.2063	1.2761	1.2610	1.2020	1.3039	1.3579	1.3903	1.4032	1.4153	1.4225	1.4379	1.4500
S	0.0000	0.254	0.9552	1.004	1.200	1.0666	1.2063	1.2761	1.2610	1.2020	1.3039	1.3579	1.3903	1.4032	1.4153	1.4225	1.4379	1.4500
M	1.4546	1.4634	1.4713	1.4769	1.4775	1.5015	1.5201	1.5247	1.5341	1.5395	1.5476	1.5591	1.5697	1.5800	1.6049	1.6092	1.6397	1.6492
N	0.0100	0.0933	0.9552	1.0143	1.1086	1.1273	1.1937	1.2032	1.2272	1.2470	1.2664	1.2794	1.2922	1.3350	1.3687	1.3785	1.3963	1.3994
C	0.0000	0.254	0.9552	1.004	1.200	1.0666	1.2063	1.2761	1.2610	1.2020	1.3039	1.3579	1.3903	1.4032	1.4153	1.4225	1.4379	1.4500
M	1.4126	1.4130	1.4602	1.4706	1.4717	1.4953	1.5062	1.5235	1.5256	1.5348	1.5532	1.5585	1.5690	1.5893	1.5975	1.5960	1.6195	1.6266
O	0.0100	0.0933	0.9552	1.0143	1.1086	1.1273	1.1937	1.2032	1.2272	1.2470	1.2664	1.2794	1.2922	1.3350	1.3687	1.3785	1.3963	1.3994
Q	0.0100	0.0933	0.9552	1.0143	1.1086	1.1273	1.1937	1.2032	1.2272	1.2470	1.2664	1.2794	1.2922	1.3350	1.3687	1.3785	1.3963	1.3994
O	1.2965	1.3019	1.3154	1.3245	1.3319	1.4011	1.4023	1.4593	1.4686	1.4983	1.5119	1.5159	1.5663	1.5948	1.6017	1.6085	1.6415	1.6415
P	0.0000	0.254	0.9552	1.004	1.200	1.0666	1.2063	1.2761	1.2610	1.2020	1.3039	1.3579	1.3903	1.4032	1.4153	1.4225	1.4379	1.4500
P	1.3172	1.3157	1.3386	1.3434	1.3510	1.3774	1.3945	1.4034	1.4085	1.4413	1.4470	1.4562	1.4942	1.5116	1.5295	1.5328	1.5365	1.5601
O	0.0000	0.254	0.9552	1.004	1.200	1.0666	1.2063	1.2761	1.2610	1.2020	1.3039	1.3579	1.3903	1.4032	1.4153	1.4225	1.4379	1.4500
U	0.0000	0.254	0.9552	1.004	1.200	1.0666	1.2063	1.2761	1.2610	1.2020	1.3039	1.3579	1.3903	1.4032	1.4153	1.4225	1.4379	1.4500
O	1.2975	1.2989	1.3100	1.3154	1.3245	1.3319	1.4011	1.4023	1.4593	1.4686	1.4983	1.5119	1.5159	1.5663	1.5948	1.6017	1.6085	1.6415
R	0.0000	0.254	0.9552	1.004	1.200	1.0666	1.2063	1.2761	1.2610	1.2020	1.3039	1.3579	1.3903	1.4032	1.4153	1.4225	1.4379	1.4500
R	1.3191	1.3145	1.3385	1.3434	1.3510	1.3774	1.3945	1.4034	1.4085	1.4413	1.4470	1.4562	1.4942	1.5116	1.5295	1.5328	1.5365	1.5601
S	0.0000	0.254	0.9552	1.004	1.200	1.0666	1.2063	1.2761	1.2610	1.2020	1.3039	1.3579	1.3903	1.4032	1.4153	1.4225	1.4379	1.4500
S	1.3769	1.4055	1.4174	1.4349	1.4520	1.4525	1.4580	1.4634	1.4706	1.4826	1.4962	1.4983	1.5155	1.5180	1.5431	1.5836	1.5982	1.6000
T	0.0000	0.254	0.9552	1.004	1.200	1.0666	1.2063	1.2761	1.2610	1.2020	1.3039	1.3579	1.3903	1.4032	1.4153	1.4225	1.4379	1.4500
T	1.4099	1.4123	1.4146	1.4450	1.4656	1.4764	1.5094	1.5119	1.5165	1.5329	1.5476	1.5506	1.5595	1.5729	1.5927	1.5960	1.6034	1.6326
U	0.0000	0.254	0.9552	1.004	1.200	1.0666	1.2063	1.2761	1.2610	1.2020	1.3039	1.3579	1.3903	1.4032	1.4153	1.4225	1.4379	1.4500
U	1.3615	1.3551	1.3876	1.4151	1.4454	1.4499	1.4533	1.4731	1.4825	1.4894	1.5029	1.5026	1.5231	1.5347	1.5654	1.5960	1.6156	1.6761
V	0.0000	0.254	0.9552	1.004	1.200	1.0666	1.2063	1.2761	1.2610	1.2020	1.3039	1.3579	1.3903	1.4032	1.4153	1.4225	1.4379	1.4500
V	1.4050	1.4054	1.4076	1.4094	1.4234	1.4295	1.4319	1.4580	1.4602	1.4686	1.4691	1.4744	1.5201	1.5592	1.5729	1.5736	1.6009	1.6300
W	0.0000	0.254	0.9552	1.004	1.200	1.0666	1.2063	1.2761	1.2610	1.2020	1.3039	1.3579	1.3903	1.4032	1.4153	1.4225	1.4379	1.4500
W	1.4311	1.4011	1.4088	1.4292	1.4316	1.4357	1.4478	1.4617	1.4626	1.4687	1.4713	1.4960	1.4963	1.5343	1.5350	1.5417	1.6329	1.6582
X	0.0000	0.254	0.9552	1.004	1.200	1.0666	1.2063	1.2761	1.2610	1.2020	1.3039	1.3579	1.3903	1.4032	1.4153	1.4225	1.4379	1.4500
X	1.4179	1.4329	1.4367	1.4409	1.4530	1.4580	1.4584	1.4742	1.4829	1.4961	1.5329	1.5373	1.5411	1.5497	1.6093	1.6266	1.6309	1.6612

Table V  
Lincoln/Mitre Sorted Distance Matrix Y - 9

[illegible]

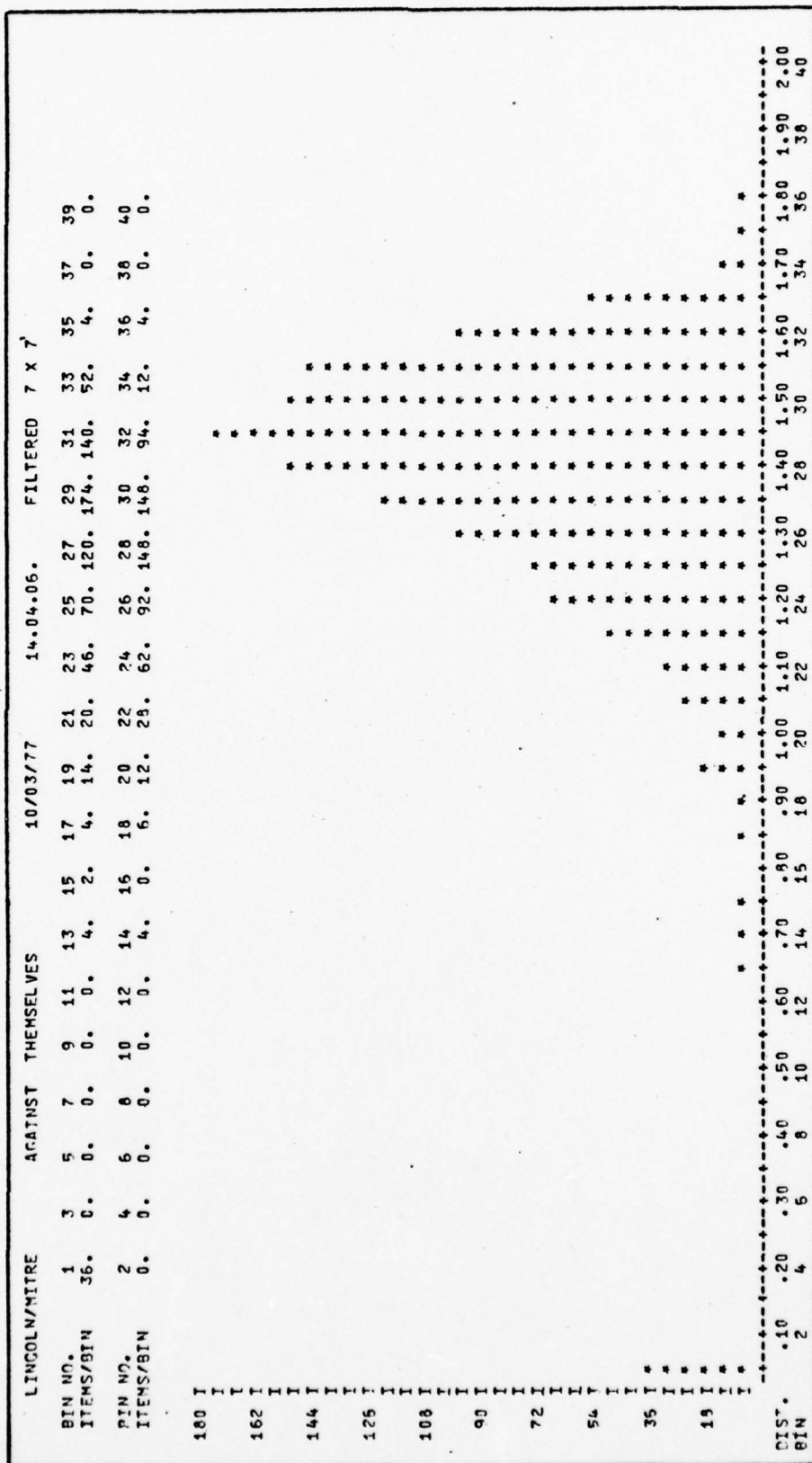


Figure 15. Histogram of Lincoln/Mitre Distances

Table VI.

## Symbol Pair Confusability Data

PAIR	DIST	PAIR	DIST	PAIR	DIST
PF	.6251	NH	.8933	83	1.0355
FP	.6251	ZE	.9008	XY	1.0532
EF	.6255	MH	.9084	G0	1.0767
RP	.6730	7T	.9382	J6	1.0828
T1	.6779	QR	.9740	6J	1.0828
1T	.6779	BD	.9751	ØW	1.1021
OU	.7098	DB	.9751	CE	1.1337
UO	.7098	Y7	.9887	SG	1.1676
LE	.8224	VW	1.0146	97	1.1737
5E	.8462	WV	1.0146	4G	1.1785
IT	.8680	KR	1.0146	28	1.1794
HN	.8933	38	1.0355	A6	1.2806

Table VII.

## Symbol Confusability Rating

1 - F	10 - 5	19 - D	28 - J
2 - P	11 - I	20 - Y	29 - 6
3 - E	12 - H	21 - W	30 - Ø
4 - R	13 - N	22 - V	31 - C
5 - T	14 - Z	23 - K	32 - S
6 - 1	15 - M	24 - 8	33 - 9
7 - U	16 - 7	25 - 3	34 - 4
8 - O	17 - Q	26 - X	35 - 2
9 - L	18 - B	27 - G	36 - A

Lincoln/Mitre set is shown in Table VII above. "F" is the most confused symbol.

Using the psychophysical data compiled from human testing of the Lincoln/Mitre font, the set can be rank ordered according to the number of errors in identification. Table VIII shows in descending order the number of errors for each symbol and Figure 16 is a plot of this data. The confusion matrix obtained from the psy-

Table VIII  
Lincoln/Mitre Psychophysical Data  
Total Errors by Rank for 6 Subjects

Rank	Symbol	Total Errors
1	P	130
2	O	99
3	1	88
4	I	84
5	F	82
6	U	75
7	S	72
8	L	72
9	5	71
10	G	59
11	E	58
12	6	57
13	B	55
14	3	50
15	J	48
16	T	47
17	8	46
18	H	35
19	4	35
20	N	32
21	Y	30
22	R	29
23	2	29
24	Z	28
25	D	26
26	W	25
27	M	24
28	0	24
29	V	23
30	X	21
31	Q	19
32	K	17
33	C	17
34	9	13
35	7	12
36	A	7

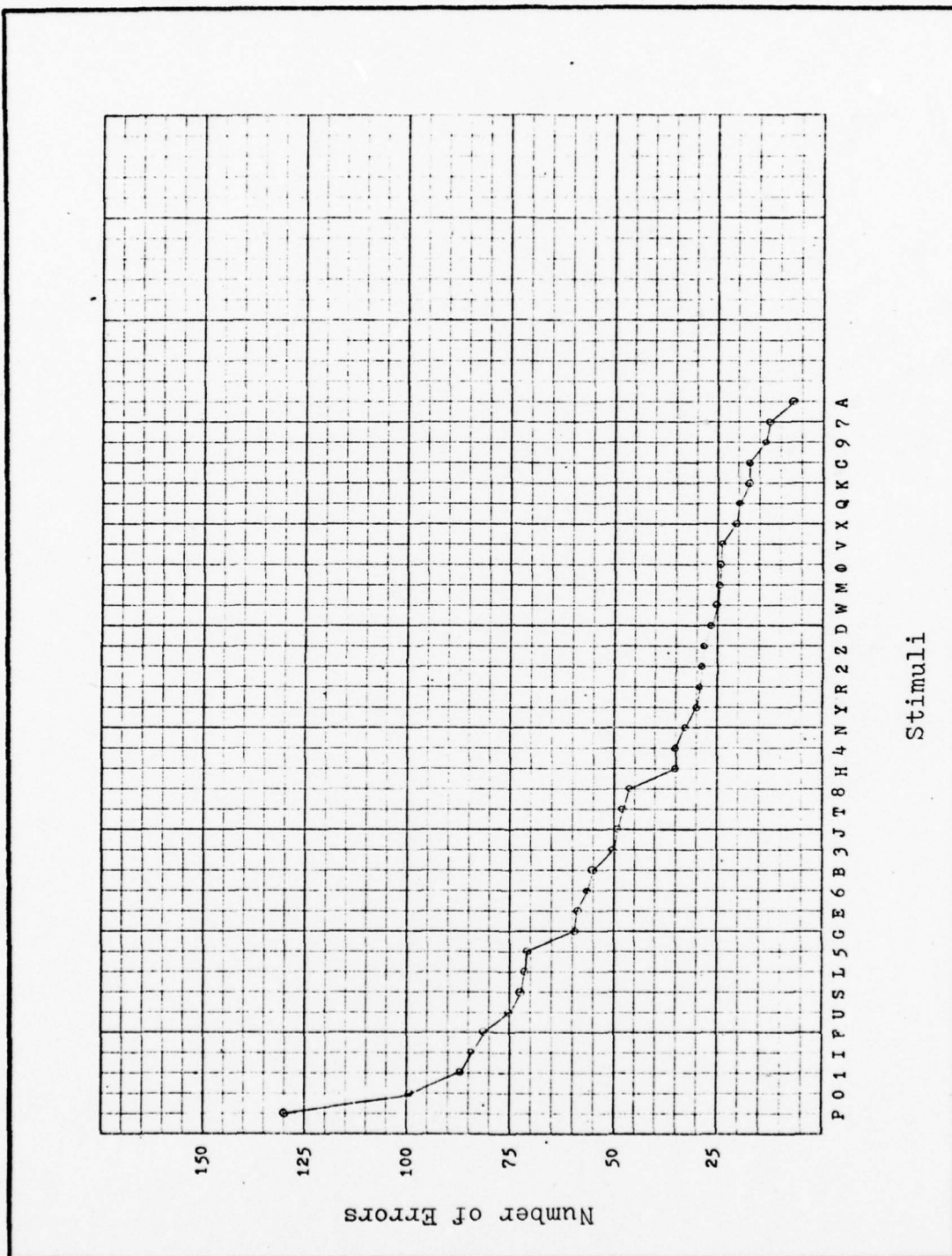


Figure 16. Lincoln/Mitre Errors vs. Stimuli

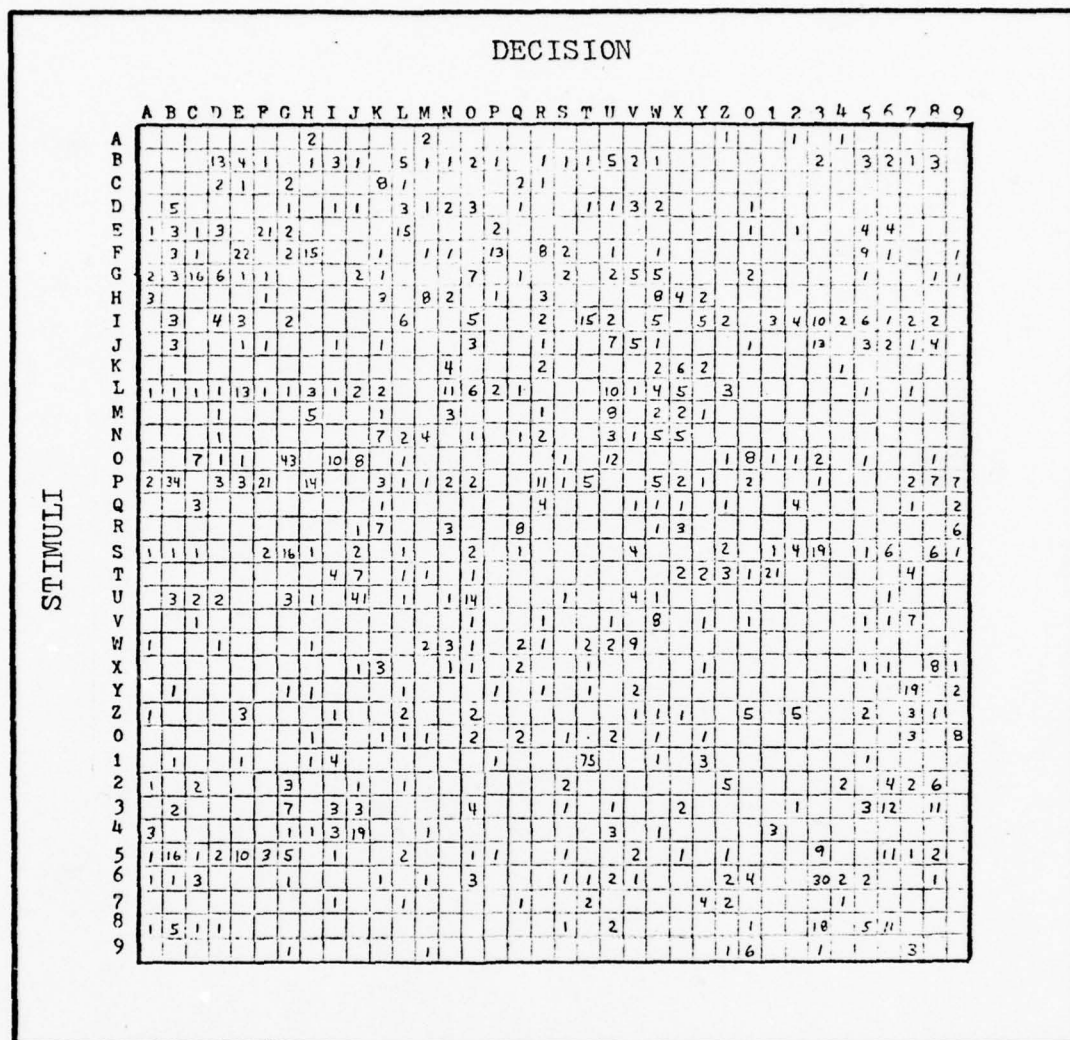


Figure 17. Confusion Matrix for Lincoln/Mitre Set

chophysical data of 6 subjects tested on the Lincoln/Mitre set is shown in Figure 17.

Another method of rating symbols compares the average distance from a symbol to all the others. The distances from a symbol to its other 35 neighbors are summed, and the mean distance is found for each symbol. The results

of this method is shown in Table IX.

#### Symbol Change Procedure

The objective of this study was to produce an alpha-numeric symbol set that is more human recognizable and with less errors between symbols. Since the Lincoln/Mitre was a highly legible set, it is chosen as the prototype set in which improvements are made. The Lincoln/Mitre font is shown in Appendix A. A nearest neighbor decision rule is used to decrease the possibility of a neighbor being classified as the prototype and to make symbols more separable. This is performed by identifying symbol pairs with small Euclidian distances and moving them further apart.

The Euclidian distance rule can also be expressed as an equivalent correlation rule. The prototype and nearest neighbor (smallest distance) compare to maximum correlation. By decreasing the correlation, this would be another means similar to increased distance movement that would make symbols less confusing.

Comparing the human error data, Table VIII to the distance rating in Table VII for the Lincoln/Mitre set, there is a good deal of agreement between human errors and small distances of separation. Eight out of the first twelve symbols identified by the Lincoln/Mitre distance rating were among the first twelve found using human data.

Table IX  
 Lincoln/Mitre  
 Ordered Mean Distance to Neighbors

Rank	Symbol	Mean Distance
1	E	1.266
2	P	1.280
3	F	1.282
4	5	1.294
5	R	1.306
6	8	1.306
7	O	1.308
8	U	1.321
9	L	1.324
10	Z	1.324
11	H	1.328
12	3	1.361
13	I	1.364
14	G	1.367
15	2	1.368
16	Q	1.375
17	7	1.376
18	B	1.378
19	N	1.378
20	J	1.380
21	C	1.382
22	S	1.384
23	K	1.387
24	T	1.388
25	W	1.395
26	V	1.396
27	Y	1.399
28	X	1.403
29	M	1.406
30	9	1.406
31	6	1.416
32	1	1.428
33	4	1.442
34	D	1.454
35	0	1.464
36	A	1.502

Symbol Change Algorithm. A symbol change algorithm was designed in which the most confusing symbols using human data results for the Lincoln/Mitre set were to be changed. Most of the errors in identification resulted from the two nearest neighbors. Using this fact, the algorithm was designed to move a confusing symbol away from its two nearest neighbors. A flowchart representing the change algorithm is shown in Figure 18.

The midpoint of the two nearest neighbors is found by the equation:

$$D_i = \frac{A_i + B_i}{2} \quad (12)$$

where  $D_i$  is the  $i$ th component of the midpoint. The symbol to be changed is moved away from this midpoint by a percentage of the distance from the midpoint and itself. The percentage of movement is called weight (WT) in the equation:

$$C_{\text{new}_i} = (C_{\text{old}_i} - D_i)WT + C_{\text{old}_i} \quad (13)$$

where  $C_{\text{new}}$  represents the new symbol after a movement. The change equation can be shown in vector notation. Figure 19 shows  $D$  as the midpoint and  $A$  and  $B$  as the two nearest neighbors. Letting  $WT = 1/10$  and  $X_1$  equal the new point  $X$  after the first movement, the vector  $\bar{V}$  equals  $1/10 \bar{XD}$ , or  $\bar{V} = 1/10(\bar{X} - \bar{D})$ . Therefore  $\bar{X}_1 = \bar{X} + 1/10(\bar{X} - \bar{D})$  or  $\bar{X}_1 = 11/10 \bar{X} - 1/10 \bar{D}$ .

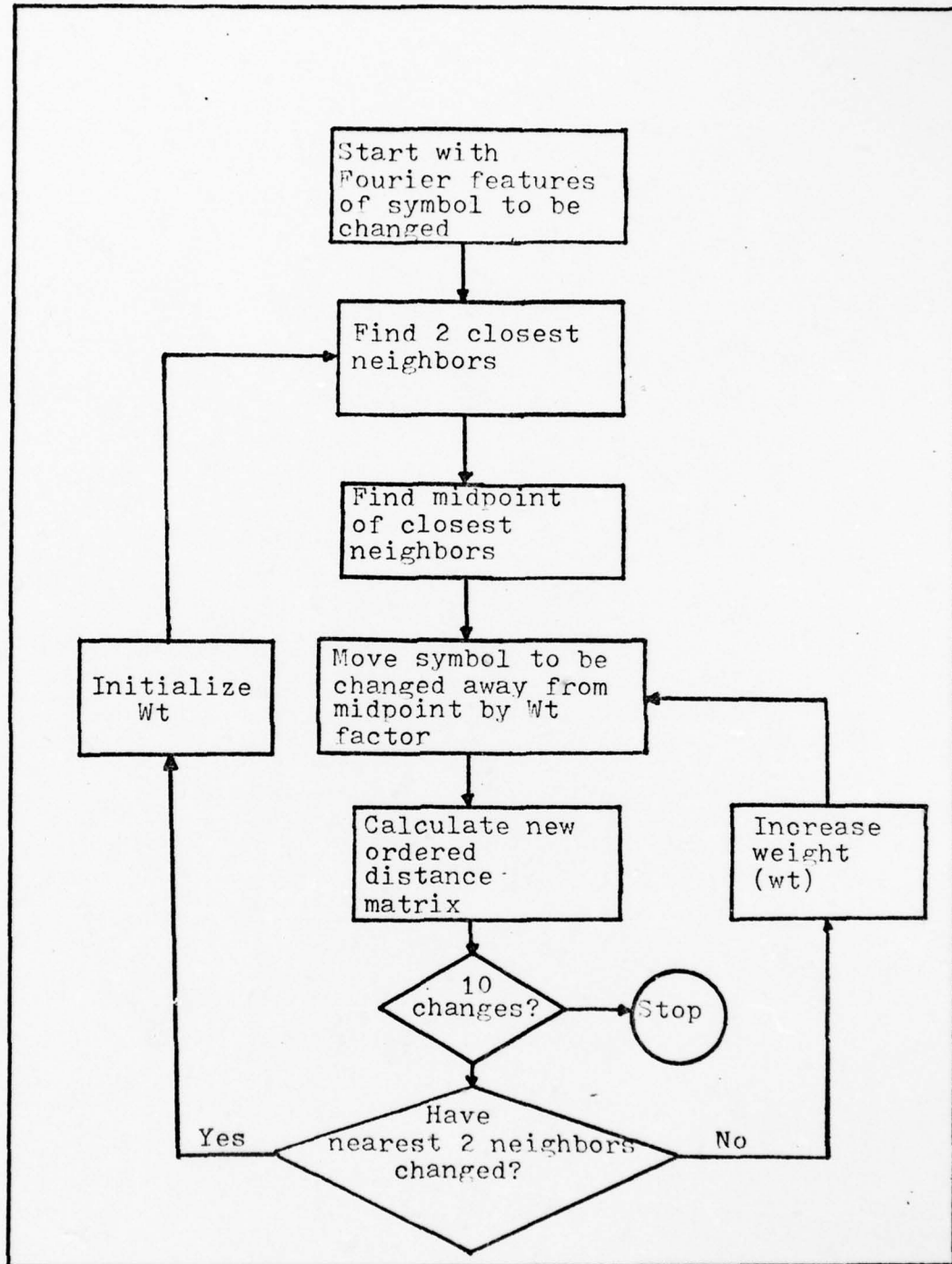


Figure 18. Symbol Change Algorithm Flow Chart

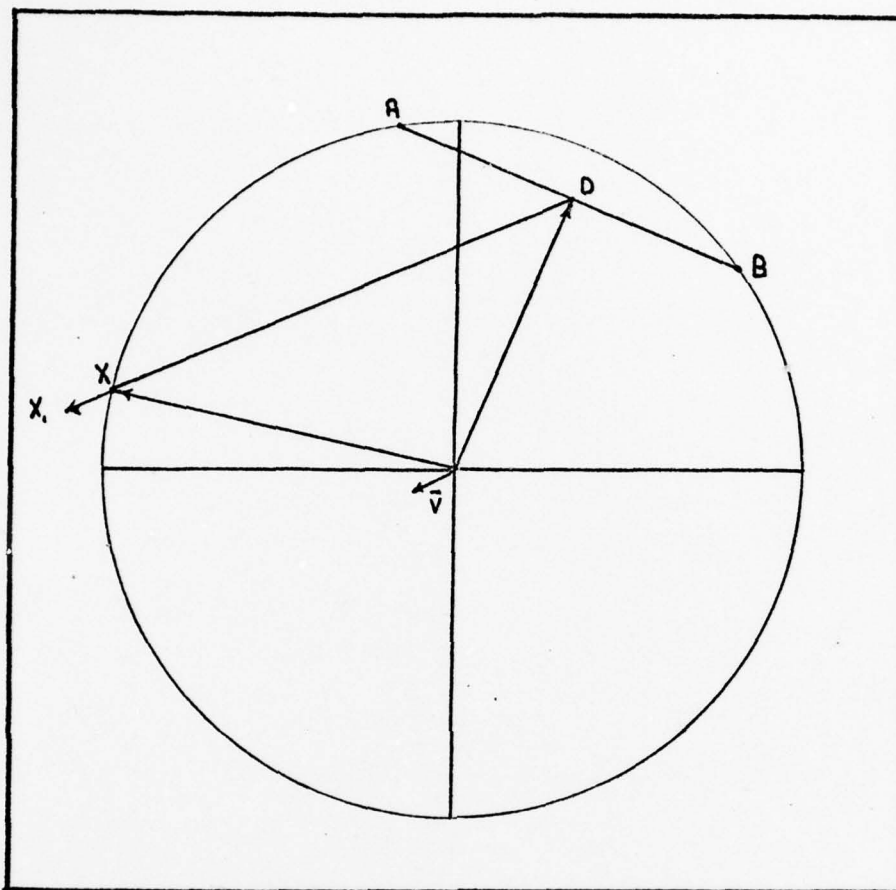


Figure 19. Vector Representation of Change Equation

Printing the Changed Symbol. Each time a new changed symbol position is found, it is again energy normalized to bring it back to the hypersphere. The inverse Fourier transform is performed and the changed symbol is printed out from a subroutine that assigns a gray level to the inverse Fourier components. The minimum and maximum inverse Fourier components are found. Gray level values ranging between 1 and 20 are then assigned

by the equation:

$$\text{gray level} = 1 + 19 \frac{(X_{m,n} - \text{Min})}{\text{Max} - \text{Min}} \quad (14)$$

where  $X_{m,n}$  is the inverse Fourier component of the  $m,n$  point in the  $30 \times 42$  matrix.

The  $30 \times 42$  matrix of gray level values is then divided evenly into  $3 \times 3$  squares. These squares will form a  $10 \times 14$  matrix, the same size as the original inputted symbol. A threshold equal to 90 is established in which the sum of each square (containing nine components) is tested. If this sum is greater or equal to the threshold, the corresponding square is assigned a one (1). If it is less, it is assigned a zero. In this way, a new  $10 \times 14$  symbol is produced.

By an overprinting procedure, a printout of the symbol is obtained. Due to filtering, the identical symbol is not reproduced, but the symbol is still recognizable. By moving the symbol further away from its two closest neighbors, its Fourier components are changed. This in turn causes a new symbol printout each time a new move is made. In the algorithm, each symbol was moved ten times and printed after each move. The two nearest neighbors were checked for changes in other symbols coming closer after the move. If a new neighbor was closer after the move, the symbol change equation would move the last location of the prototype being

changed away from the new midpoint of these new neighbors. An example using the letter "P" and its closest neighbors "F" and "R" is shown in Figure 20 on the next page. After the 10th movement, the curved part of the "P" is highlighted and indicates that more information should be placed in the loop of the "P." The final (10 X 14) "P" that was obtained is shown compared with the original in Figure 21.

Lincoln/Mitre	Final Set
11111111--	11111111--
111111111-	11--11111-
11-----111	11----1111
11-----11	11----1111
11-----11	11----1111
11-----111	11----1111
111111111-	11--11111-
11111111--	11111111--
11-----	11-----
11-----	11-----
11-----	11-----
11-----	11-----
11-----	11-----
11-----	11-----

Figure 21. "P": Lincoln/Mitre and Final Set

The symbol change procedure was also applied to a transformed symbol without filtering. All the Fourier components of the symbol were used in the change algorithm. The results of printing the symbol "P" from its inverse Fourier coefficients after 5 movements is shown in Figure 22. Both the filtered and non-filtered

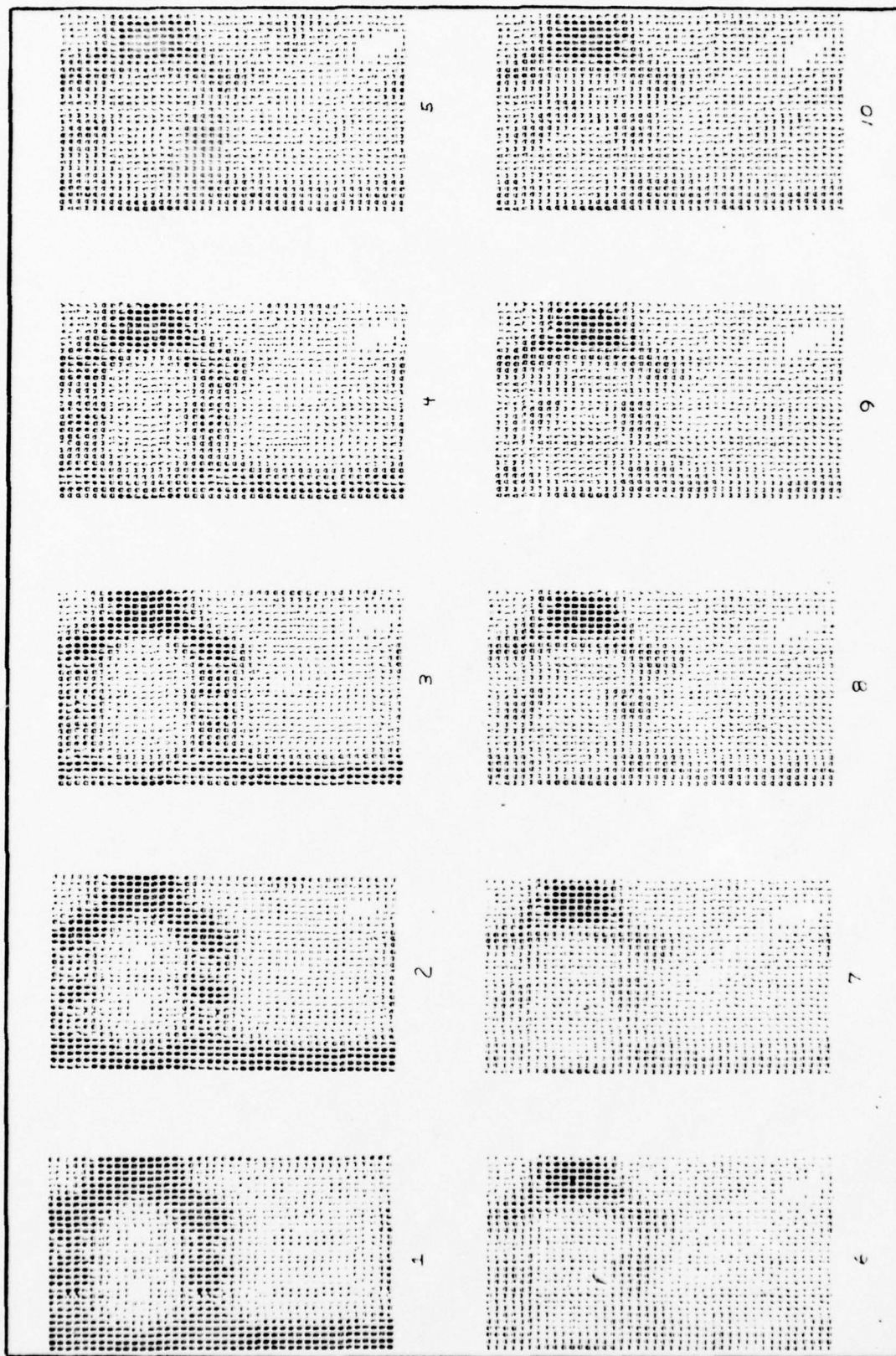


Figure 20. Ten Movements of Lincoln/Mitre "P" from two closest neighbors

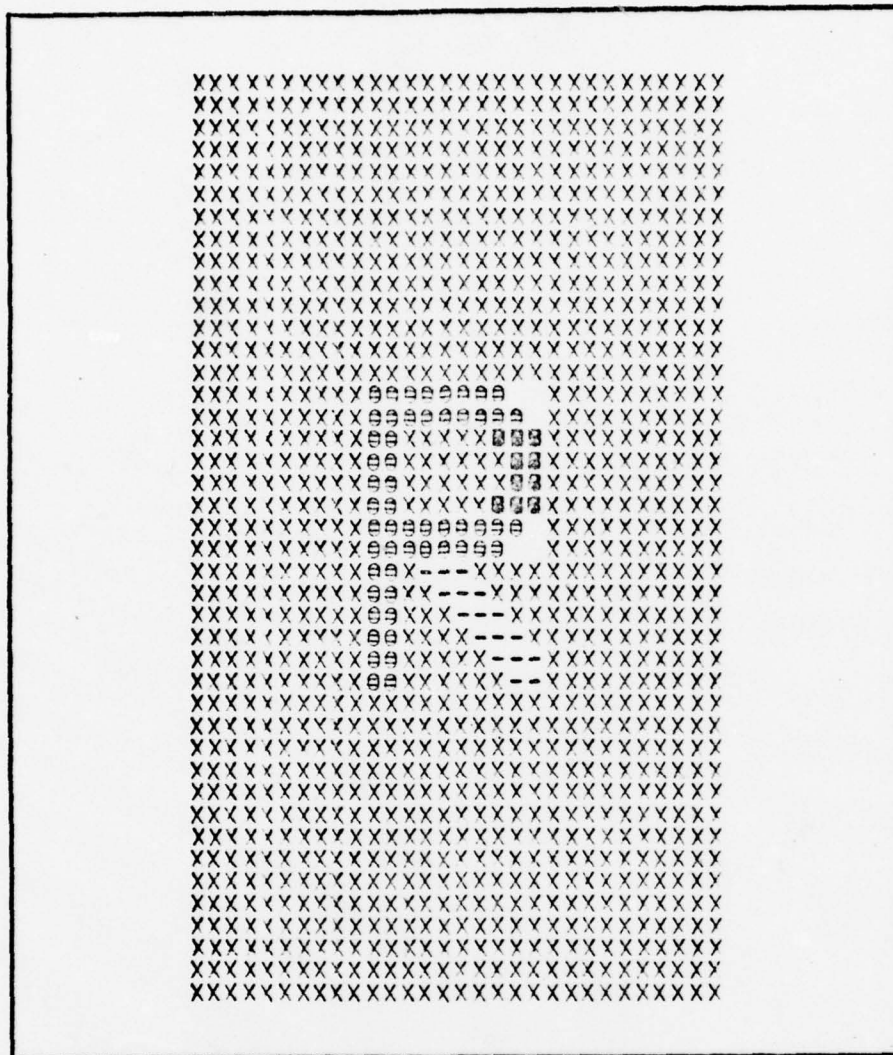


Figure 22. Lincoln/Mitre "P" after 5 Movements  
with no Filter

procedure demonstrated similarities in identifying which "P" pixel elements are stressed the most after the same amount of change.

After each movement of the symbol in the feature space, there is a continuous increase in the distance between the prototype and its two nearest neighbors.

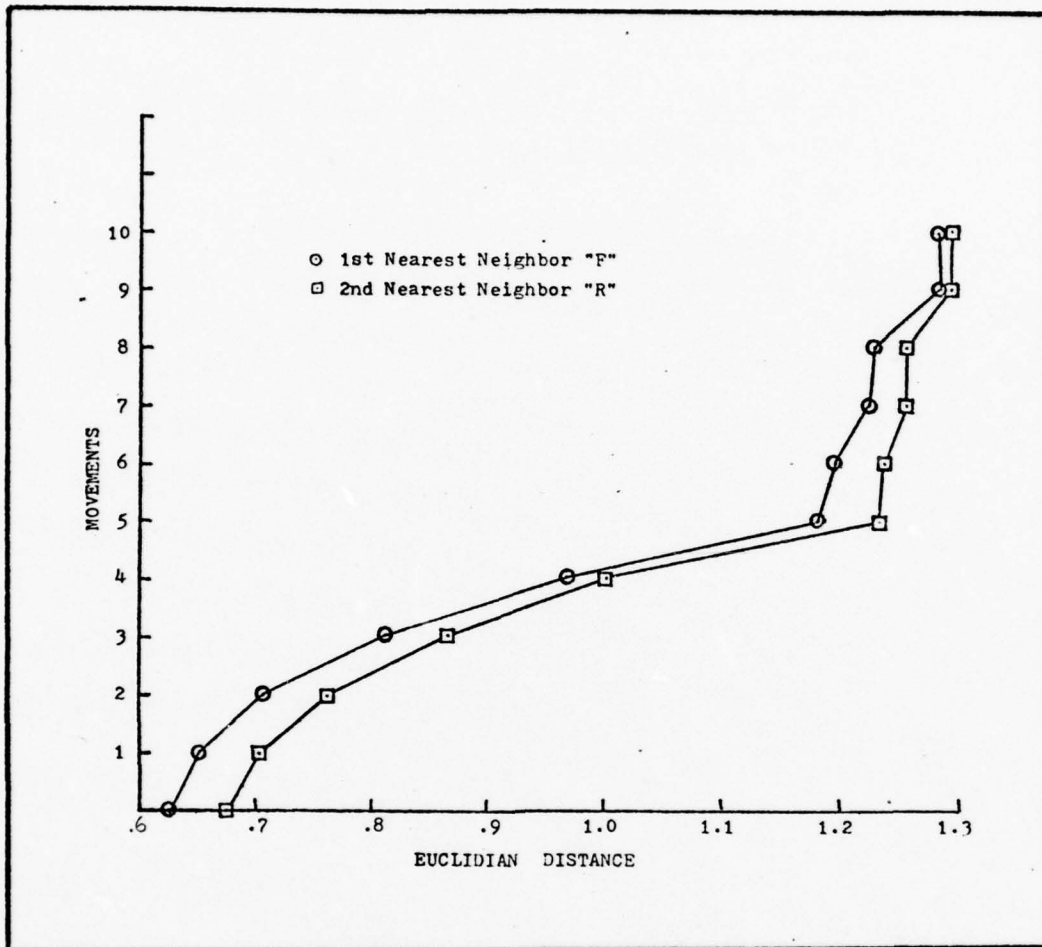


Figure 23. "P" Movement from Nearest Neighbors

Table X shows the first 6 nearest neighbors of the Lincoln/Mitre "P" after 10 movements. Figure 23 shows how the two nearest neighbors "F" and "R" moved after each change of the Lincoln/Mitre "P." Most of the distance spread for the first two neighbors occurred in the first five moves. On the fifth move both the "F" and "R" were replaced by other symbols as the nearest neighbors. For

Table X  
Lincoln/Mitre "P" after 10 Movements

Movement	Neighbor with Distance					
	1st	2nd	3rd	4th	5th	6th
1	F .6515	R .7010	E .9455	H .9620	O 1.1218	Z 1.1235
2	F .7097	R .7616	H .9816	E .9879	O 1.1162	Z 1.1352
3	F .8116	R .8659	H 1.0215	E 1.0620	O 1.1124	8 1.1562
4	F .9693	R 1.0241	H 1.0949	O 1.1197	8 1.1554	E 1.1774
5	O 1.1528	8 1.1747	B 1.1753	F 1.1801	H 1.2095	R 1.2323
6	B 1.1924	F 1.1946	O 1.2003	8 1.2220	H 1.2235	9 1.2358
7	O 1.2115	B 1.2228	F 1.2250	H 1.2374	8 1.2442	9 1.2445
8	F 1.2285	H 1.2427	9 1.2458	O 1.2510	M 1.2563	R 1.2568
9	9 1.2382	B 1.2557	2 1.2676	O 1.2682	V 1.2695	7 1.2810
10	M 1.2545	O 1.2672	V 1.2731	2 1.2774	F 1.2806	9 1.2813

weight equal to one-tenth, there was enough information after 10 movements to determine which features will make the prototype more recognizable from its two nearest neighbors. It must be remembered, that changing a symbol may in fact cause it to come closer to other symbols

in the set and therefore negate the results of the original change. Once a new symbol set is found, its ordered Euclidian distance matrix is calculated and compared to the original set. All symbols in the set are checked to verify how much of an increase or decrease in distance between each symbol and its two nearest neighbors. Symbol pairs with decreased distances were then reconsidered for further change. It is noted that slight changes in a symbol could cause the nearest neighbors to change and also reduce distances in some cases.

This particular procedure was repeated for the most confusing of the Lincoln/Mitre symbols. A new symbol set was found based on information obtained from the changed symbol printout. Basic criteria was always to try to increase the original Lincoln/Mitre symbol distances. A total of 11 different sets were run with the final set 11 showing the best increase in distance between prototype and nearest neighbors. Set 11 is shown in Appendix B. A total of 18 symbols were changed from the original Lincoln/Mitre font.

#### IV. Testing

Psychophysical testing of the newly generated font, referred to as set 11, was conducted in conjunction with the Multimode Matrix Display Office of the Air Force Flight Dynamics Laboratory. The objective of the testing was to determine the legibility of set 11 compared to the Lincoln/Mitre font. A font's legibility is determined by the total errors made in identification under similar viewing conditions.

##### Subjects

A total of two male personnel served as subjects. Each subject had 20/20 or corrected 20/20 vision, and none reported any evidence of visual abnormalities. One of the subjects had participated in a previous experiment dealing with font legibility.

##### Stimuli

The test stimuli consisted of the letters A-Z and numbers 0-9 in both the Lincoln/Mitre and in set 11. The stimuli were photographed on 35mm slides in the form of transparent 10 X 14 dot matrix arrays on an opaque high-density black background. There was a total of 80 slides in each slide tray which included two sets of each font and 8 additional symbols.

One dot was centered on the viewing screen to act as a fixation point for the subject and to indicate that

another slide was in place. Prior and following each test stimulus, a 19 msec stimulus mask was flashed on the screen. The mask was a bright light of homogenous illumination that filled the complete stimulus viewing area of the 10 X 14 array. Masking of a test stimulus by a flash of light is termed blanking (Ref 13;91). The mask and stimulus time were the same for each subject. Figure 24 shows the trial sequence.

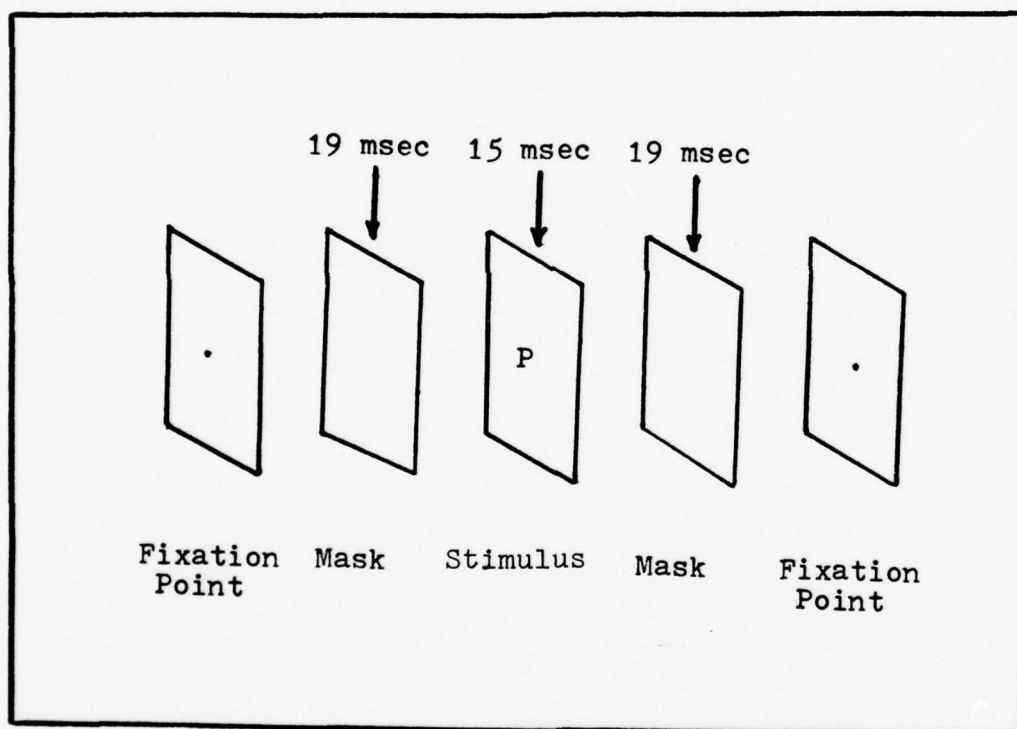


Figure 24. Psychophysical Testing Sequence

Masking techniques are used to force errors to occur by deteriorating the viewing conditions. With continued practice a subject's performance increases.

If all fonts achieve a 100% level, then there is no disparity between them to judge their legibility. This high performance level occurred when a visual noise mask of a random array of white dots on a dark background was used. For this reason, the light masking was used to obtain a 70-80 percent starting error rate. Masking interrupts the signal to the brain and changes the signal to noise ratio of the stimulus by increasing the noise component. The mask that follows each stimulus helps to decrease the effects of the after images (Ref 13:94).

#### Apparatus

The testing facility consisted of a room for the subject and a room for the experimenter and testing equipment. A 12.7 cm X 15.2 cm viewing screen was built into the connecting wall between the rooms. The subjects were seated approximately one meter in front of the screen. Subjects wore a two-way intercom headphone to enable verbal communication with the experimenter. A subject would initiate each experimental trial by pressing the microswitch which would activate the equipment.

All stimuli were rear-projected onto the viewing screen. The stimuli exposure time was operated by an electronic shutter controlled by a Iconix projection tachistoscopic system. A Kodak Carousel projector with random access was used to project the test stimuli.

### Procedure

Before the first testing session, each subject was briefed on the task involved. They were told to press the microswitch in order for the mask-stimulus to be flashed on the screen. They would respond into the microphone with the symbol they identified, and guess if they were undecided. Before each testing period, the subjects were permitted to study the fonts to insure familiarity of stimuli symbols. Each font of 36 characters was contained on two sheets of paper 21.5 cm X 35.5 cm. Each symbol was in 10 X 14 dot-matrix configuration with 2.5 cm X 3.5 cm in the X-Y direction.

After each subject was familiar with the test stimuli; the subject was seated in the darkened room. He was given several minutes for his eyes to adjust to the room. For each test period, each subject would start with a different font and with both the Lincoln/Mitre and set 11 font being tested. In between trials the experimenter would reposition the slide tray at random positions. The subject was given a practice run consisting of 160 slides on the first font to be tested. The second font tested normally would show better results due to the learning received from the first font. By each subject testing the fonts in different orders, a compensation for the learning effects was achieved. The experimental conditions were carefully controlled

to insure extraneous factors would not be introduced into the study.

A total of 36 test trials were conducted over a 3 week period of 12 testing days. Each subject was tested 3 times during each testing day. Over 10,300 symbols were tested by both subjects over the testing period.

Accurate measurements were taken to specify precisely all the test viewing conditions. The average intensity of each dot was 5 footlamberts (fL) and it varied for each symbol. For a given viewing distance  $d$ , the visual angle  $\theta$ , subtended by a symbol of size  $h$  can be calculated using the equation:

$$\theta = 2 \tan^{-1} (h/2d) \quad (15)$$

For a viewing distance of 1 meter and a symbol size on the screen of 6.5 cm high by 1.0 to 4.6 cm wide, results in a viewing angle of  $3.72^\circ$  vertically and  $0.57^\circ$  to  $2.64^\circ$  horizontally. The percent active area is given by the equation:

$$\text{percent active area} = \frac{\text{emitter size}}{(\text{emitter spacing})^2} \times 100 \quad (16)$$

Emitter spacing is the distance between the centers of adjacent dots, while emitter size is the area of each dot. The approximate diameter of each dot was 0.4 cm. The spacing between dots was 0.5 cm with resulting active area equal to 50%.

## V. Results

### Computer Algorithm Results

The symbols of the final set 11 that were changed from the original Lincoln/Mitre set are indicated by a underline in Appendix B. A total of 18 symbols were changed. The histogram for the final set 11 inter-prototype Euclidian distances is shown in Figure 25. The Lincoln/Mitre symbols with the smaller distance separation, which is represented by the left side of the histogram, were spread further apart. By comparing the histogram of the Lincoln/Mitre set to that of the final set, the distance shifting can be verified. The minimum distance for the final set is .8307 which is the distance between "P" and "F." The original distance for the worst pair of the Lincoln/Mitre set was .6251, also for "P" and "F." The mean distance between all symbols also increased from 1.3706 to 1.3755 in the final set. The standard deviation was .1537 in the final set and .1766 in the Lincoln/Mitre.

Taking a closer look at the distance spread, the symbol change objective based on Euclidian distance was achieved in moving the closest symbols in order to increase the distance between them and the other symbols in the set. A comparison of the number of symbols in each distance increment and its associated bin number

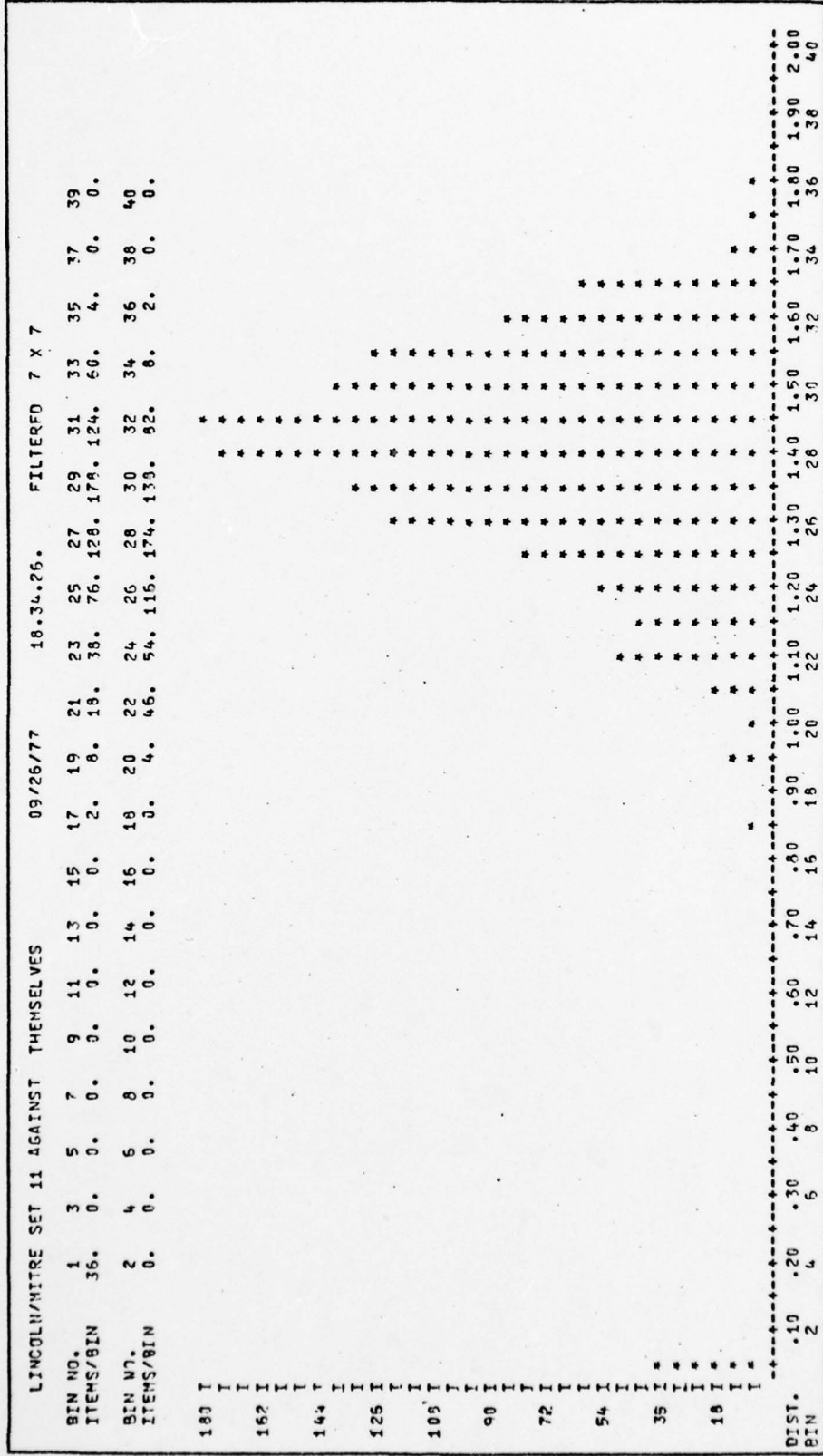


Figure 25. Histogram for Final Set 11 Distances

is shown in Table XI.

In the first 20 bins, which includes distances up to and including 1.00, the final set had a total of 14 symbols whose nearest neighbors were within this distance range; this compares to 46 symbols in the original Lincoln/Mitre font.

Table XII shows each symbol and the distance to its nearest neighbor for both the Lincoln/Mitre and final set. In the final set, 33 symbols showed an increase in the distance to their nearest neighbor from the original set. The 10 symbols that showed the most change were the E,O,U,L,R,T,1,5,P,F in that order. These ten symbols, but not in the exact order, were the same symbols in the first ten ranking by symbol confusability.

#### Psychophysical Testing Results

The psychophysical results indicated that the test was more difficult in the early trials. Near the end of the test a ceiling effect was being approached and performance was nearly 85%. The final test set 11 showed a significant advantage over the Lincoln/Mitre set in the early part of the test as is shown in the cumulative percent correct by trial in Figure 26. Under higher stress conditions, the final set seemed to perform better and as the test got easier, both sets performance asymptotically approached the same level. A learning effect was associated with the test and showed

Table XI  
Bin Number Data for Lincoln/Mitre and Final Set

Bin Numbers	Range	Lincoln/Mitre Symbols	Final Set Symbols
1	0.0 - .05	0	0
2	.05 - .10	0	0
3	.10 - .15	0	0
4	.15 - .20	0	0
5	.20 - .25	0	0
6	.25 - .30	0	0
7	.30 - .35	0	0
8	.35 - .40	0	0
9	.40 - .45	0	0
10	.45 - .50	0	0
11	.50 - .55	0	0
12	.55 - .60	0	0
13	.60 - .65	4	0
14	.65 - .70	4	0
15	.70 - .75	2	0
16	.75 - .80	0	0
17	.80 - .85	4	2
18	.85 - .90	6	0
19	.90 - .95	14	8
20	.95 - 1.0	12	4
21	1.0 - 1.05	20	18
22	1.05 - 1.10	28	46
23	1.10 - 1.15	46	38
24	1.15 - 1.20	62	54
25	1.20 - 1.25	70	76
26	1.25 - 1.30	92	116
27	1.30 - 1.35	120	128
28	1.35 - 1.40	148	174
29	1.40 - 1.45	174	178
30	1.45 - 1.50	148	138
31	1.50 - 1.55	140	124
32	1.55 - 1.60	94	82
33	1.60 - 1.65	52	60
34	1.65 - 1.70	12	8
35	1.70 - 1.75	4	4
36	1.75 - 1.80	4	2
37	1.80 - 1.85	0	0
38	1.85 - 1.90	0	0
39	1.90 - 1.95	0	0
40	1.95 - 2.00	0	0

Table XII  
Lincoln/Mitre and Final Set  
Distance to Nearest Neighbor

Symbol	Nearest Neighbor		Difference
	Lincoln/Mitre	Final Set	
A	1.2806	1.2806	0
B	.9761	1.0539	.0778
C	1.1337	1.1266	-.0071
D	.9761	1.0698	.0937
E	.6255	.9614	.3359
F	.6261	.8307	.2046
G	1.0767	1.0698	-.0069
H	.8933	.9082	.0149
I	.8530	1.0248	.1718
J	1.0828	1.0828	0
K	1.0305	1.0963	.0613
L	.8224	1.0963	.2739
M	.9084	1.0119	.1035
N	.8933	.9082	.0149
O	.7098	1.0303	.3205
P	.6251	.8307	.2056
Q	.9470	.9735	.0265
R	.6730	.9093	.2363
S	1.1676	1.1676	0
T	.6779	.9040	.2261
U	.7098	1.0303	.3205
V	1.0146	1.0193	.0047
W	1.0146	1.0193	.0047
X	1.0532	1.0532	0
Y	.9887	1.0142	.0255
Z	.9008	1.0248	.1240
0	1.1021	1.1366	.0345
1	.6779	.9040	.2261
2	1.1794	1.1794	0
3	1.0355	1.0595	.0240
4	1.1785	1.1785	0
5	.8462	1.0595	.2133
6	1.0828	1.0828	0
7	.9382	1.0288	.0906
8	1.0355	1.0539	.0184
9	1.1737	1.1075	-.0662

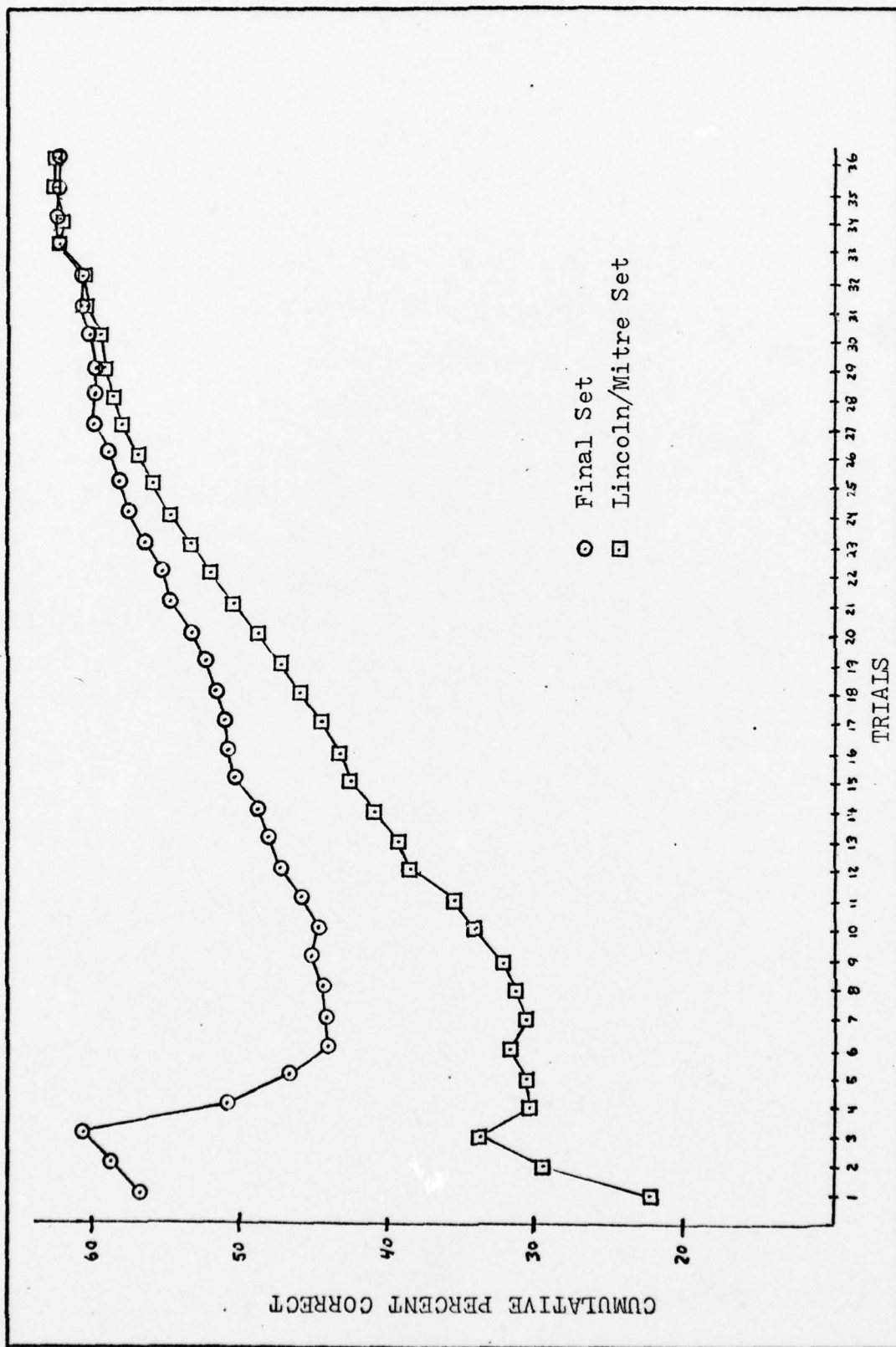


Figure 26. Cumulative Percent Correct by Trial

a decrease in the percentage of errors as the test continued.

Of the two subjects tested, one had been previously tested on the Lincoln/Mitre font over a 7 month period. As expected, he performed approximately 4% better on the Lincoln/Mitre font. The other subject, without any prior learning of the Lincoln/Mitre font, performed approximately 4% better on the final set 11.

Since only 18 symbols were different in the two sets, a comparison of how well the changed symbols performed between fonts would be interesting information. Table XIII shows the number of errors in both sets for the changed symbols only. The changed symbols identification results for both subjects was 67% correct in the final set and only 57.5% in the Lincoln/Mitre font. The test favored the new changed symbols by 9.5% with an overall increase in distance to their nearest neighbors. For symbols that were identical in both sets, the Lincoln/Mitre set was favored by 12.1%. What is the disparity in such a case when symbols are the same but in different sets? One reason could be imperfections in the dot size and arrangement of dots on the slide from one font to the other. This would cause variations in light intensity and contrast between the symbols. Different error rates for identical symbols may mean that recognition performance depends on the learning effect

Table XIII  
Changed Symbols Total Errors for Both Fonts

Symbol	Identification Errors	
	Lincoln/Mitre	Final Set
C	51	23
D	81	86
E	54	56
H	58	31
I	75	25
K	90	47
L	35	41
N	40	37
O	92	53
P	89	48
R	72	60
T	46	49
U	83	69
W	17	23
Z	44	39
3	37	50
5	70	29
7	58	85
Total	1102	856

for the entire font.

Some changed symbols like the "T" and the "L" had increased thickness or stroke width with slightly higher error rates. Although the symbol change algorithm had emphasized the features that were thickened, the increased thickness seemed to increase legibility of the

symbol up to a maximum value; wider strokes then tended to cause more errors to occur in identification.

The psychophysical results should only be considered as a pilot study in the determination of the legibility between the Lincoln/Mitre font and the set 11 font. More conclusive results can be made with further investigation and testing using more subjects over a longer test period.

## VI. Conclusions and Recommendations

### Conclusions

The results in Chapter V indicated that the legibility of the Lincoln/Mitre alphanumeric symbol set was improved with a new font which demonstrated better performance when the identification task was most difficult. Also important is the fact that the 18 changed symbols in the new set 11, which had an overall greater Euclidian distance between prototype and nearest neighbors, were less confusing than the Lincoln/Mitre set. These results support the hypothesis that an inter-prototype Euclidian distance matrix, produced from a low-pass filtered, two-dimensional discrete Fourier transform, may be of merit as a human visual perception model. The larger the inter-prototype distance spread, the lower the recognition errors and more dissimilar the symbols.

The symbol change algorithm was designed to move a prototype away from its two closest neighbors and indicate which Fourier component features were the most significant after symbol changes. Using this information, the changed symbol's spatial image was used to digitize a new symbol with greater distance separation from it to its nearest two neighbors.

This thesis is only one approach to finding more legible alphanumeric symbol sets. The symbol change

algorithm effectively decreases the discriminability error between symbols based on increased Euclidian distance measures. Table XIV summarizes the entire procedures of the algorithm used to arrive at new symbols.

#### Recommendations

It is recommended for further study that the outlined procedures of Table XIV be used to change every Lincoln/Mitre symbol. Design a new legible alphanumeric set with a greater distance spread between symbols. Use the same procedure to produce other symbol sets not including alphanumerics.

It is suggested that the final set 11 be tested using a new test paradigm in which the error rate is standardized for each subject during each trial by applying different masking levels. Also it is desired to increase the number of subjects to 10 and increase the number of trials to 50. Reaction time may be another testing parameter besides subject errors.

The present process of photographing each symbol onto a slide has a tendency to cause random variations in the quality of each slide and in the shape of each symbol. This in turn could cause identification errors that have not been accounted for. The implementation of a computer controlled system rather than the tachistoscope system would enhance not only the accuracy

Table XIV  
Symbol Algorithm

---

1. Digitalize each symbol by sampling the intensity pattern of the symbol by use of the flying spot scanner or other practical method.
2. Center symbol in zero filled matrix array.
3. Using FOURT subroutine, transform each digitally represented symbol into its Fourier spatial components.
4. Extract features by low-pass filtering each transformed symbol.
5. Energy normalize each transformed symbol to place on the hypersphere.
6. Compute the Euclidian distance between each filtered transformed pair and print the Euclidian distance matrix for the complete set.
7. Order distances and print out ordered Euclidian distance matrix for complete set.
8. Use symbol change procedure to move prototype away from two closest neighbors.
9. Take inverse Fourier transform of changed symbol and obtain its spatial image.
10. Using the changed symbol's spatial image, digitalize a new symbol.
11. Repeat steps 2-7 to verify increased Euclidian distance matrix for changed prototypes.

but also increase the availability of meaningful results.

Finding other methods in which the changed symbol's spatial image can be interrupted to give exact pixel elements for the new symbol is another area where research is needed.

There are a variety of other factors besides symbol shape that effect legibility that can be explored. Shurtleff (Ref 23) has experimented with many legibility factors to include symbol brightness, contrast, illumination, exposure time, spacing, size, stroke width, and viewing area. Other factors such as noise, blur, vibration, and repetition rate effect symbol legibility.

Appendix E also suggest further study in using the symbols of legible sets to form suboptimal sets based on Euclidian distance. These sets can then be analyzed for "optimum" conditions.

## Bibliography

1. Ankeney, Larry A. The Classification of Chinese Characters by Spatial Filtering. Unpublished thesis. Wright-Patterson Air Force Base, Ohio: Air Force Institute of Technology, March 1971. AD 722852\*.
2. Campbell, F.W. and D.G. Robson. "Application of Fourier Analysis to the Visibility of Gratings." Journal of Physiology, 181:551-566 (1968).
3. Carl, J.W. Generalized Harmonic Analysis for Pattern Recognition: A Biologically Derived Model. Unpublished thesis. Wright-Patterson Air Force Base, Ohio: Air Force Institute of Technology, September 1969. AD 862441\*.
4. Carl, J.W. and C.F. Hall. "The Application of Filtered Transforms to the General Classification Problem." IEEE Transactions on Computers, C-21: 785-790 (July 1972).
5. Cooley, J.W. and J.W. Tukey. "An Algorithm for Machine Calculation of Complex Fourier Series." Mathematics of Computation, 19: 297-301 (April 1965).
6. Dailey, K.G. and F.S. Sutton. An Automatic Speech Recognition System Using a Vocoder Input. Unpublished thesis. Wright-Patterson Air Force Base, Ohio: Air Force Institute of Technology, March 1972. AD 742441\*.
7. Duda, Richard O. and Peter E. Hart. Pattern Classification and Scene Analysis. New York: John Wiley and Sons, 1973.
8. Gagnon, Roger A. Detection and Identification of Objects Embedded in Cluttered Fields: A Reconnaissance Problem. Dissertation. Wright-Patterson Air Force Base, Ohio: Air Force Institute of Technology, May 1975. ADA 017187\*.
9. Guyton, A.C. Textbook of Medical Physiology (Fourth Edition). Philadelphia: W. B. Saunders Co., 1971.
10. Ginsburg, A.P. Psychological Correlates of a Model of the Human Visual System. Unpublished thesis. Wright-Patterson Air Force Base, Ohio: Air Force Institute of Technology, May 1970. AD 731197\*.

11. Goble, Larry G. Filtered 2-Dimensional Discrete Fourier and Walsh Transform Correlation with Recognition Errors and Similarity Judgements. Dissertation. Ann Arbor, Michigan: University of Michigan, 1975.
12. Goodman, Joseph W. Introduction to Fourier Optics. San Francisco: McGraw-Hill Book Company, 1968.
13. Haber, Ralph N. Information-Processing Approaches to Visual Perception. University of Rochester: Holt, Rinehart and Winston, Inc., 1969.
14. Honigfeld, A.R. Radar Symbolology: A Literature Review. Technical Memorandum 14-64. Aberdeen Proving Grounds, Maryland: Human Engineering Laboratories, 1964. AD 461180\*.
15. Johnson, James A. An Algorithm to Generate an Optimally Human-Separable Symbol Set. Unpublished thesis. Wright-Patterson Air Force Base, Ohio: Air Force Institute of Technology, December 1976. ADA 034030\*.
16. Kabrisky, Matthew. A Proposed Model for Visual Information Processing in the Human Brain. Urbana, Illinois: University of Illinois Press, 1966.
17. Kanal, Laveen. "Patterns in Pattern Recognition: 1968-1974" IEEE Transactions on Information Theory, IT-20: 697-722 (November 1974).
18. Parrent, George B. Jr. and B.J. Thompson. Physical Optics Notebook. Redondo Beach, California: Society of Photo-optical Instrumentation Engineers, 1971.
19. Peters, Gregory L. Human Factors of Dot Matrix Displays. Unpublished technical report. Wright-Patterson Air Force Base, Ohio: Air Force Flight Dynamics Laboratory, February 1976.
20. Radoy, Charles H. Pattern Recognition by Fourier Series Transformations. Unpublished thesis. Wright-Patterson Air Force Base, Ohio: Air Force Institute of Technology, March 1967. AD 561801\*.
21. Scanlan, L.A. and W.L. Carel. Human Performance Evaluation of Matrix Displays: Literature and Technology Review. AMRL-TR-76-39. Wright-Patterson Air Force Base, Ohio: Aerospace Medical Research Laboratory, June 1976. ADA 029932\*.

22. Shurtleff, D.A. "Legibility Research." Proceedings of the Society for Information Display, 15-2: 41-51 (Summer 1974).
23. Shurtleff, D. Design Problems in Visual Displays-Part I, Classical Factors in the Legibility of Numerals and Capital Letters. ESD-TR-66-62, United States Air Force, Electronic Systems Division, Hanscom Field, Bedford, Mass., June 1966. AD 636414\*.
24. Tallman, Oliver H., II. The Classification of Visual Images by Spatial Filtering. Dissertation. Wright-Patterson Air Force Base, Ohio: Air Force Institute of Technology, June 1969. AD 858866\*.
25. Vanderkolk, R.J., et al. "Dot Matrix Display Symbolology Study." AFFDL-TR-75-72. Wright-Patterson Air Force Base, Ohio: Air Force Flight Dynamics Laboratory, July 1975.
26. Yu, Francis T. S. Introduction to Diffraction, Information Processing, and Holography. Cambridge, Massachusetts: The MIT Press, 1973.

\* Available from the Defense Documentation Center,  
Cameron Station, Alexandria, Virginia 22314

## Lincoln/Mitre Set

74

[illegible]



Final Set 11

```

1111111111
:1111111111
 11      1111
 11      1111
 11      1111
 11      1111
1111111111
1111111111
 11      1111
 11      1111
 11      1111
 11      1111
1111111111
1111111111

```

[illegible][illegible]

```

1111111111
1111111111
1111
1111
11111111111111
11111111111111
11111111111111
11111111111111
1111
1111
1111
1111
11111111111111
11111111111111
11111111111111

```

```

1111111111111111
1111111111111111
111
111
111
111
1111111111111111
1111111111111111
111
111
111
111
111

```

```

      1 1 1 1
    1 1 1 1 1
  1 1 1   1 1 1
 1 1       1 1
1 1
1 1
1 1
1 1
1 1
1 1   1 1 1 1 1
1 1   1 1 1 1 1
1 1       1 1
1 1 1   1 1 1
  1 1 1 1 1
    1 1 1

```

```

11      11
11      11
11      11
11      11
11      11
11      11
11111111111111
11111111111111
11111111111111
11      11
11      11
11      11
11      11
11      11

```

```

111111111
111111111

    11
    11
    11
    11
    11
    11

1111111111111
1111111111111

```

[illegible]

```

11
11
11
11
11
11
11
11
11
11
11
11
11
11
11
11
11
11
11
11

```



79 .

## Appendix C

ASCII, Namel, Huddleston, and IBM Sets

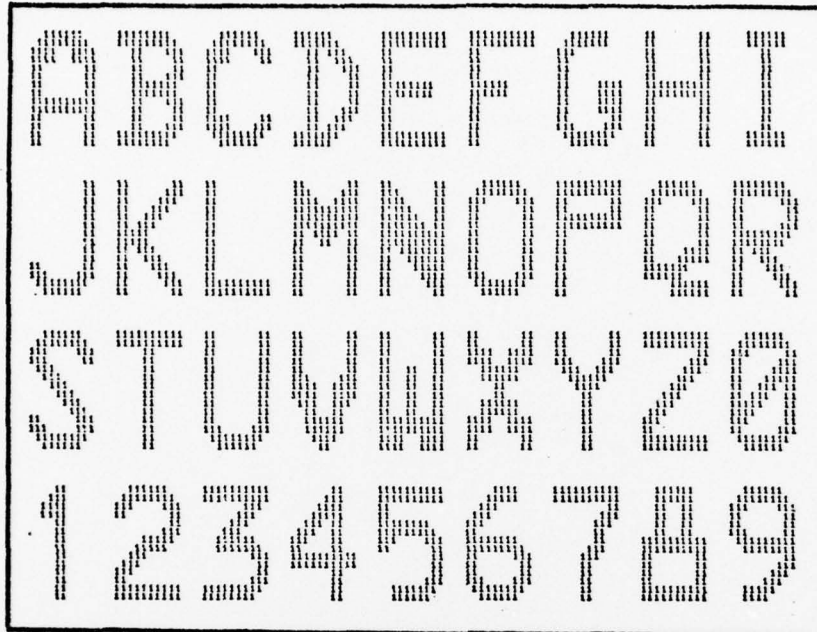
### ASCII

A	B	C	D	E	F	G	H	I
J	K	L	M	N	O	P	Q	R
S	T	U	V	W	X	Y	Z	0
1	2	3	4	5	6	7	8	9

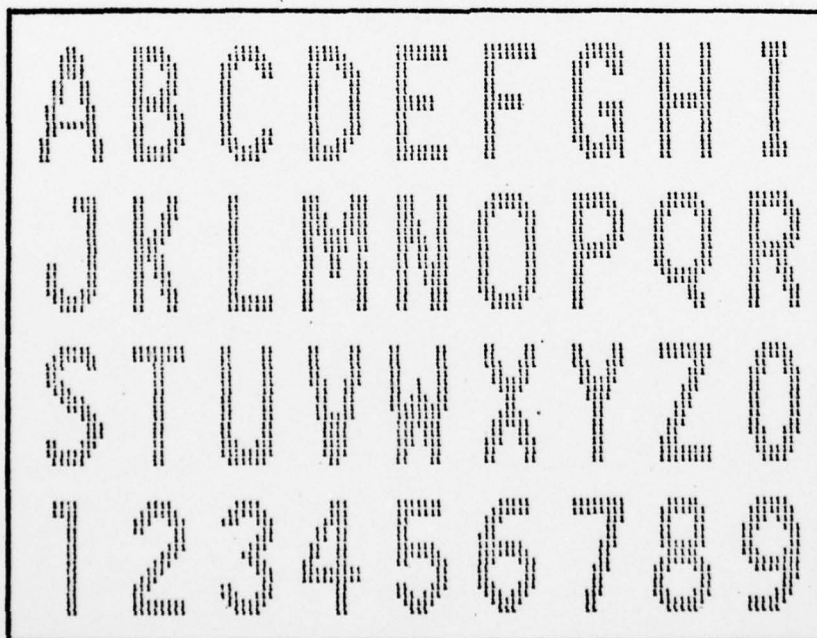
### Namel

A	B	C	D	E	F	G	H	I
J	K	L	M	N	O	P	Q	R
S	T	U	V	W	X	Y	Z	0
1	2	3	4	5	6	7	8	9

Huddleston



IBM



## Appendix D

### Fourier Transform in Fraunhofer Diffraction

Diffraction is the deviation of light from its straight-line propagation resulting from the interaction with the edges of obstacles it encounters in its path. Diffraction can be classified as either Fraunhofer or as Fresnel; the type depends on the distances of the light source and the viewing screen from the diffracting screen. Fraunhofer diffraction is said to occur when the diffraction screen is far from the light source and viewing screen, and there is only a small fraction of the wavelength between lines drawn from the viewing point or source to all points of the aperture (Ref 26:24,25).

Fraunhofer diffraction displays a Fourier transform pattern on the far field from a diffracting aperture. The Fourier transform is given by:

$$\psi(x,y) = \iint A(\xi,\eta) e^{\frac{ik}{f}(\xi x + \eta y)} d\xi d\eta \quad (17)$$

where  $A(\xi,\eta)$  describes the amplitude and phase of the field across the aperture and  $\psi(x,y)$  describes the field in the focal plane.

Consider a rectangular aperture centered on the axis of the  $\xi$  and  $\eta$  plane. Let the width equal to  $2a$

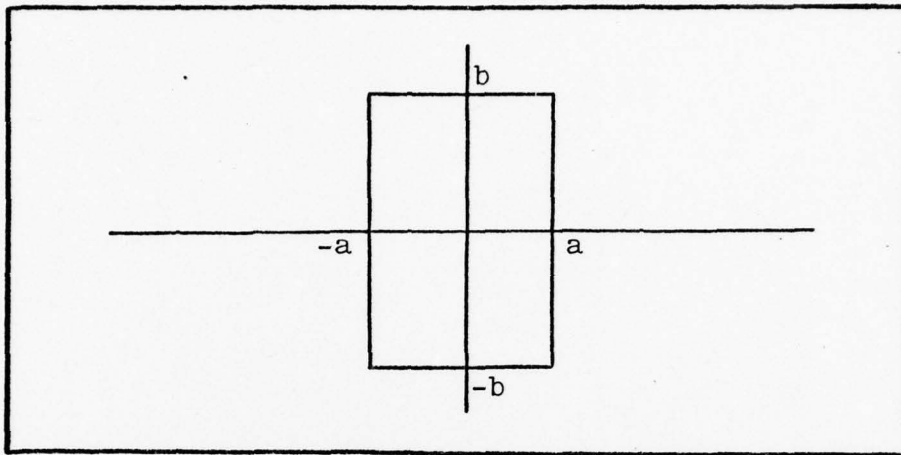


Figure 27. Rectangular Aperture

and the length equal to  $2b$  as shown in Figure 27 above. Then the Fourier transform of  $A(\xi, \eta)$  that occurs in the observation plane will be:

$$\psi(x, y) = \int_{-a}^a \int_{-b}^b A(\xi, \eta) e^{\frac{ik}{f}(\xi x + \eta y)} d\xi d\eta \quad (18)$$

and after the integration is performed the following is obtained:

$$\psi(x, y) = 4Aab \operatorname{sinc}\left(\frac{kax}{f}\right) \operatorname{sinc}\left(\frac{kby}{f}\right) \quad (19)$$

Figure 28 shows a cross section of the Fraunhofer diffraction pattern along the X axis (Ref 18:4,5).

Using monochromatic light from a laser source and the setup shown in Figure 29 on the next page, the Fraunhofer diffraction pattern for a wire mesh aperture was photographed on the back focal plane of the imaging lens. The pattern is shown in Figure 30. The wire mesh

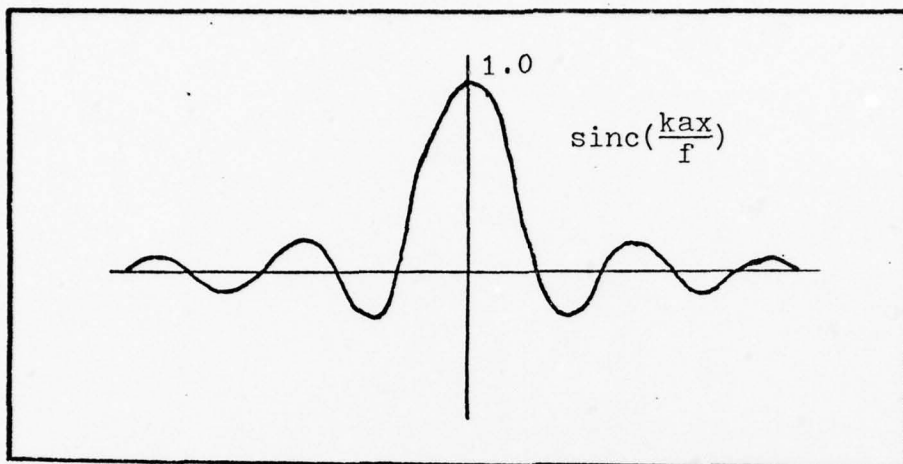


Figure 28. Cross Section of Fraunhofer Diffraction Pattern along X Axis

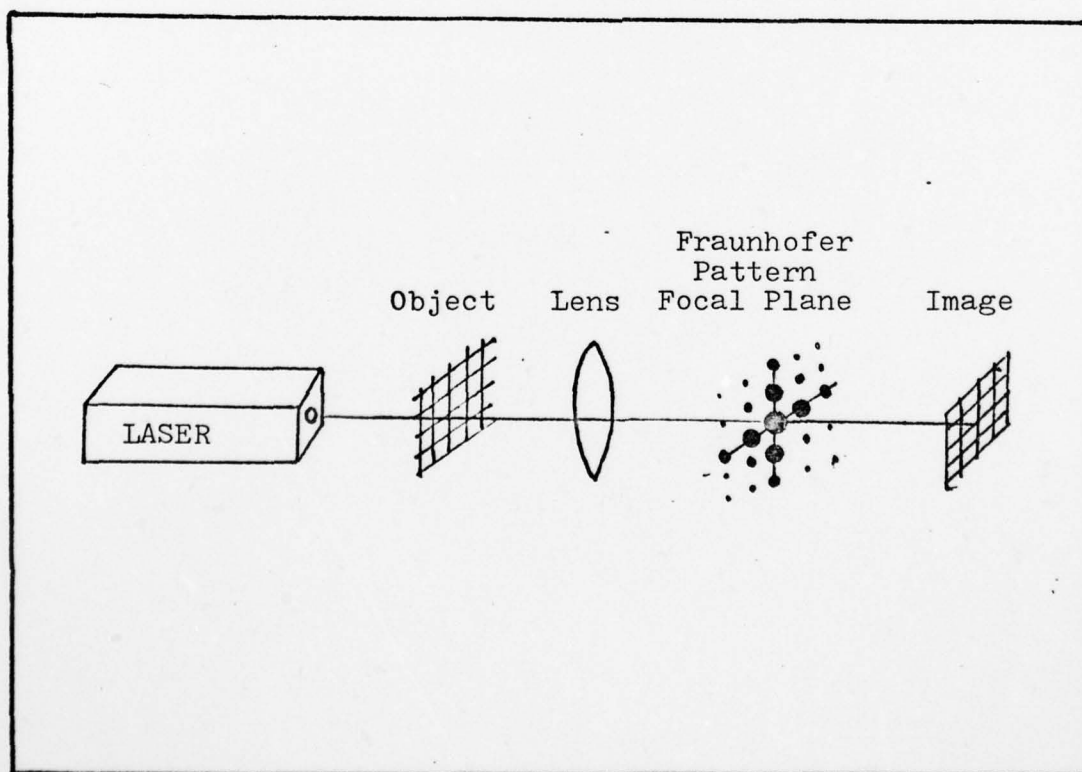


Figure 29. Fraunhofer Diffraction Setup

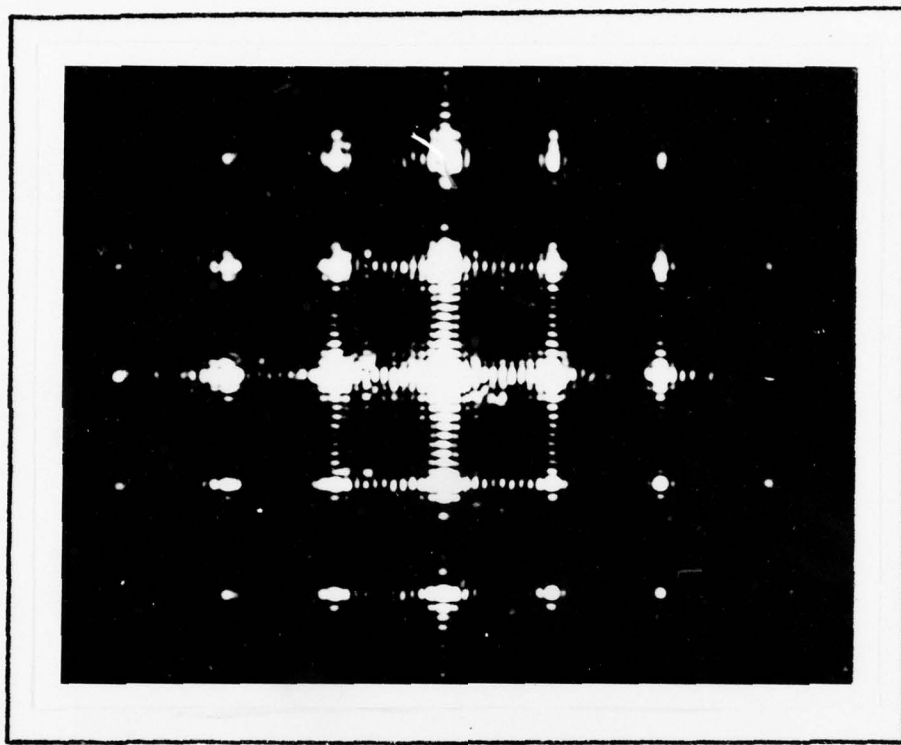


Figure 30. Fraunhofer Diffraction Pattern of Wire Mesh

image is restructured from the various Fourier components and is photographed at the image plane in Figure 31.

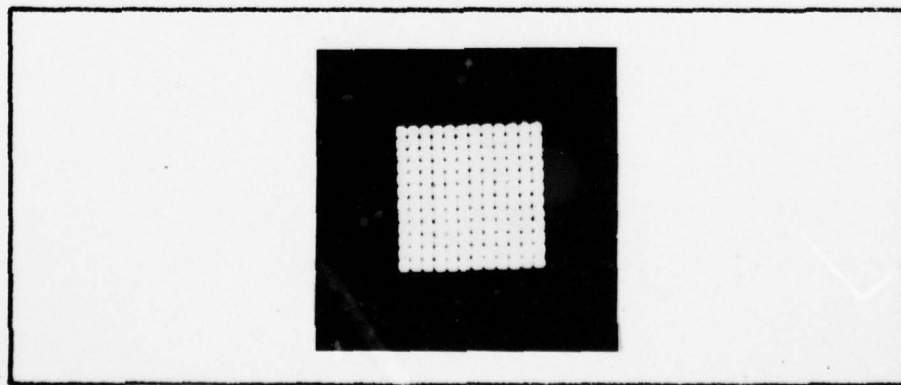


Figure 31. Restructured Wire Mesh Image

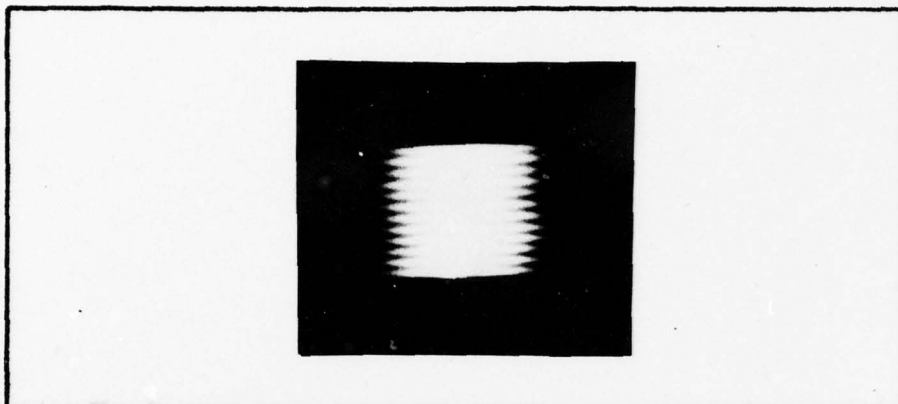


Figure 32. Horizontal Image Using Vertical Slit

Spatial filtering techniques can be demonstrated by placing a narrow vertical slit in the focal plane. This slit will pass only a single row of Fourier components. The corresponding image contains only the horizontal structure of the wire mesh as shown in Figure 32. The opposite is true for the horizontal slit filter.

The number "4" was photographed onto a slide and was used in place of the wire mesh. The Fraunhofer diffraction pattern of the "4" was obtained. An adjustable iris was used to eliminate all the spatial frequencies greater than the first harmonic and the filtered diffraction pattern was photographed in Figure 33. The reproduced image was a blurry "4" which was double exposed with the diffraction plane and is also shown in Figure 33. The high frequency components that yield edge information are filtered out. This preserves only

AD-A053 447

AIR FORCE INST OF TECH WRIGHT-PATTERSON AFB OHIO SCH--ETC F/G 1/4  
THE DESIGN OF AN OPTIMUM ALPHANUMERIC SYMBOL SET FOR COCKPIT DI--ETC(U)  
DEC 77 L F BUSH

UNCLASSIFIED

AFIT/GE/EE/77-11

NL

2 OF 2

AD  
A053447



END

DATE  
FILMED

6 -78

DDC



the basic form of the original image.

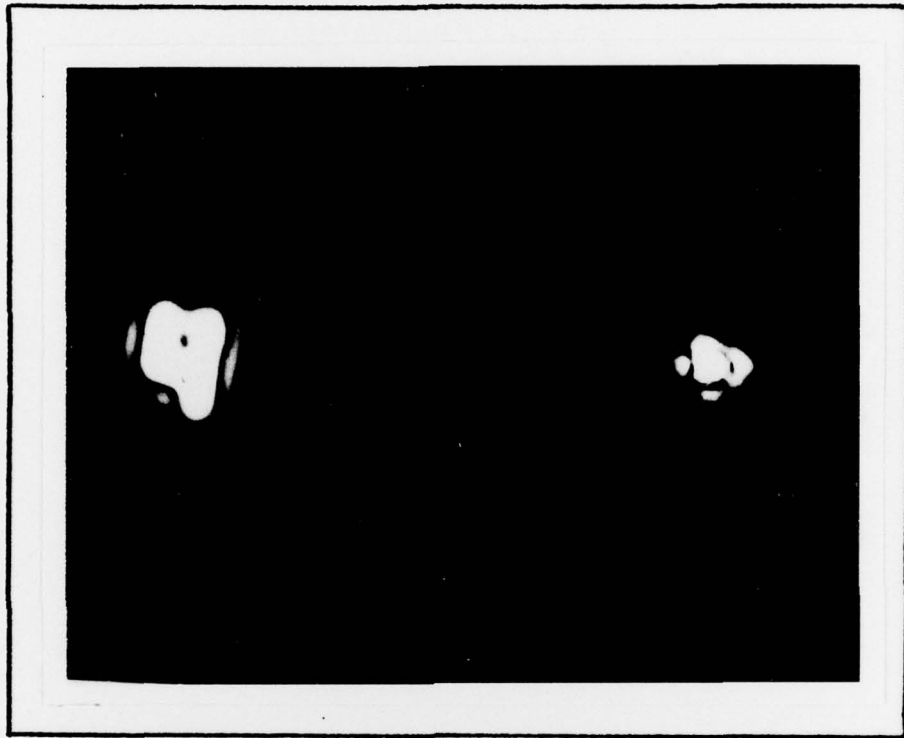


Figure 33. Number "4" with Spatial Filter

## Appendix E

### Optimization of Legible Sets Using Distance Measure

For N alphanumeric symbol sets, each set consisting of 36 prototypes, A - Z and 0 - 9, the most "optimal" set is defined as the combination 36 symbol alphanumeric set with the maximum Euclidian distance between every prototype. To manually find this set given a  $36N$  by  $36N$  Euclidian distance matrix is normally infeasible due to the large combinations of possible symbol sets; therefore, a method is desired that will limit the number of investigations and at the same time find candidates consisting of suboptimal sets.

The first procedure described develops a new symbol set from prototypes of several legible fonts. Any candidate set, in which the distance between any two symbols is less than an established minimum distance, is excluded from consideration. The objective is to find combination sets that will have an increased overall Euclidian distance from each symbol to its nearest neighbor.

In this process, a computer algorithm is used, in which all symbols have been spatially filtered and their corresponding Fourier coefficients locate each symbol in a higher order space. An Euclidian distance matrix was

then calculated between all prototypes.

A 36N by 36N matrix of Euclidian distance values would take up a large amount of computer space. Since the distance data is symmetrical about the diagonal, this information is utilized to only store half of the values. An array is generated which contains the distance and a pointer to its location in the original matrix. This array of distances with location symbol pairs is then sorted from largest to smallest.

Once the sorting is complete, the search begins to find the first complete set with the largest distance between symbols. No distance is accepted smaller than the minimum distance which is called Zmin. A counter I is used and initilized to one. The following steps are performed:

1. Starting at the Ith point in the sorted array, the symbol pair at that position becomes the first two symbols for the suboptimal set called array IA. If the distance of the pair at I is not greater than Zmin, the process will stop.
2. The next lower pair of symbols in the sorted array is checked. If the distance for this pair is less than Zmin, then a complete set cannot be found. If one of the symbols is already in array IA, the procedure will be continued but that symbol will not be stored in array IA.

3. Another check is made to confirm that a symbol class already placed in array IA is removed from further consideration. For example, if a "R" of one set had been chosen, then no more "R"s are needed. In this case, the procedure would proceed to the next pair of the sorted array.

4. Before storing a new symbol in array IA, the distance between it and all other symbols in array IA are checked. If all distances are greater than  $Z_{min}$ , that symbol is accepted into the suboptimal set. If the distance is less than  $Z_{min}$ , the procedure starts over at step 2 again.

5. Once a complete suboptimal set is found, it is printed along with its distance matrix. The counter I is increased by one either when a complete set is found or when after all possible checks, a complete set cannot be formed. The process will then start over at step 1.

The final suboptimal sets obtained will have a minimum interprototype distance equal or greater than the  $Z_{min}$  value. Test can then be performed on these suboptimal sets to determine which ones are optimal under different conditions. Different statistical methods can be applied to discriminate between sets.

Another procedure suggested uses a symbol set mean distance between all prototypes as a measurement criterion.

Given N alphanumeric symbol sets, the one with the largest mean distance is used as the model set. Starting with the first symbol, the "A" is exchanged for an "A" of another set and a new mean distance is calculated. In turn, after all the "A"s of all the sets are tested, the "A" that gives the highest overall mean is saved in the model set. The procedure then continues for the "B"s and so on until all symbols have been tested and a final new symbol set obtained.

The above procedures are only attempts at finding "optimal" sets using distance measures. The actual choice of "optimal" sets depends upon the peculiar nature of each problem and the manner in which its algorithm is implemented.

## Appendix F

### Window Effect on the Distance Matrix

Prior to taking the Fourier transform of a symbol, each symbol was centered in a zero filled window that was three times its size. The window was used to eliminate or reduce edge effects, aliasing and leakage conditions that could result from the periodic nature of the Fourier transform. What effect does the window have on the Euclidian distance matrix? This question was answered by comparing the distance matrix for a symbol set using 10 X 14 symbols centered in a window to one obtained for a symbol set whose symbols occupied the entire 30 X 42 window space. Fourier analysis and low-pass filtering were performed on both sets.

The ASCII symbol set shown in Appendix C was used. Each symbol in the set was also enlarged three times its size by an algorithm that assigned nine "1"s for each digitalized "1" of the original 10 X 14 symbol. In this way a new 30 X 42 ASCII symbol set was developed. The bigger symbols had more of a staircase effect due to the scaling problem that is created by the digitalizing process. This in turn can induce some error into the distance matrix since it is not an identical enlargement of the original symbol but a digital repre-

sentation.

The ordered Euclidian distance matrix was calculated for the ASCII set with and without a window. Part of the ordered distance matrix for both sets, A - L, is shown in Table XV and in Table XVI. Checking the first two nearest neighbors for all symbols, only the letter "E" showed a difference and this was in the 2nd neighbor. The window effect was insignificant in changing the position of the nearest neighbors and showed only slight deviations in positions for the entire set.

Table XV

[illegible]

Table XVI

25 X OF 1135

### Vita

Larry F. Bush was born on 9 March 1946 in Harrisburg, Pennsylvania. He graduated from Cedar Cliff High School in 1964 and attended the United States Air Force Academy from which he received a Bachelor of Science degree in Basic Sciences in June, 1970. Upon graduation, he was commissioned in the Regular United States Air Force. He completed Undergraduate Navigator Training at Mather Air Force Base, California, in 1971. Other assignments include Squadron Section Commander of 1002nd Organization Maintenance Squadron at Andrews Air Force Base, Maryland and Headquarters Squadron Commander at U-Tapao Airfield, Thailand. He entered the Masters Program in the School of Engineering, Air Force Institute of Technology, in June 1976.

Permanent Address: 3572 Clayton Road  
San Jose, California

UNCLASSIFIED

SECURITY CLASSIFICATION OF THIS PAGE (When Data Entered)

14 REPORT DOCUMENTATION PAGE		READ INSTRUCTIONS BEFORE COMPLETING FORM
1. REPORT NUMBER AFIT/GE/EE/77-11	2. GOVT ACCESSION NO.	3. RECIPIENT'S CATALOG NUMBER
4. TITLE (and Subtitle) THE DESIGN OF AN OPTIMUM ALPHANUMERIC SYMBOL SET FOR COCKPIT DISPLAYS.		5. TYPE OF REPORT & PERIOD COVERED 9 Masters thesis MS Thesis
7. AUTHOR(s) 10 Larry F. Bush Captain, USAF		6. PERFORMING ORG. REPORT NUMBER
9. PERFORMING ORGANIZATION NAME AND ADDRESS Air Force Institute of Technology (AFIT-EN)		8. CONTRACT OR GRANT NUMBER(s)
11. CONTROLLING OFFICE NAME AND ADDRESS Air Force Flight Dynamics Laboratory (FGR) Air Force Systems Command Wright-Patterson AFB, Ohio 45433		10. PROGRAM ELEMENT, PROJECT, TASK AREA & WORK UNIT NUMBERS
14. MONITORING AGENCY NAME & ADDRESS (if different from Controlling Office)		12. REPORT DATE 11 Dec 1977
		13. NUMBER OF PAGES 12 106 P.
		15. SECURITY CLASS. (of this report) Unclassified
16. DISTRIBUTION STATEMENT (of this Report) Approved for public release; distribution unlimited		
17. DISTRIBUTION STATEMENT (of the abstract entered in Block 20, if different from Report)		
18. SUPPLEMENTARY NOTES Approved for public release; IAW AFR 190-17 JERRAL F. GUESS, Captain, USAF Director of Information		
19. KEY WORDS (Continue on reverse side if necessary and identify by block number) Pattern Recognition Fourier Transform Spatial Filtering Spatial Frequencies Symbol Legibility		
20. ABSTRACT (Continue on reverse side if necessary and identify by block number) The purpose of this study was to design an alphanumeric symbol set with improved legibility which could be implemented as a standardized set for cockpit displays. Pattern recognition theory was applied in which the two-dimensional, discrete, Fourier transform was used to obtain the feature space for each symbol. Spatial low-pass filtering techniques were employed and a decision rule was used based on the maximum nearest prototype Euclidian distance		

012225

hc

UNCLASSIFIED

SECURITY CLASSIFICATION OF THIS PAGE(When Data Entered)

between symbols. A symbol change algorithm was developed in which symbols were moved away from their two closest neighbors in the transformed domain. Lincoln/Mitre, a highly legible font, was used as the initial prototype set. A new alphanumeric symbol set was designed with 18 changed symbols that had an overall greater distance spread between nearest neighbor symbols. The Lincoln/Mitre and a new test set were psychophysically tested with results indicating a 9.5% better performance for the changed symbols over the original Lincoln/Mitre symbols.

UNCLASSIFIED

SECURITY CLASSIFICATION OF THIS PAGE(When Data Entered)